Small State Enterprise "Laser Physics"

Membrane – based primary mirrors with diffractive optical coatings for aberration sensing and compensation

Final report of the Contract
F61775-99-WE053

Director SSE "Laser Physics"

_____ **Dr.L.V. Kovalchuk**

Scientific Leader

_____ **Dr. V.E. Sherstobitov**

Principal Investigator

_____ **Dr. S.A. Dimakov**

St.Petersburg
2000

REPORT DOCUMENTATION PAGE

Form Approved OMB No. 0704-0188

1. AGENCY USE ONLY (Leave blank)	2. REPORT DATE	3. REPORT TYPE AND DATES COVERED
	2000	Final Report

4. TITLE AND SUBTITLE

Membrane-Based Primary Mirrors With Diffractive Optical Coatings For Aberration Sensing And Compensation

5. FUNDING NUMBERS

F61775-99-WE

6. AUTHOR(S)

Dr. Vladimir E. Sherstobitov

7. PERFORMING ORGANIZATION NAME(S) AND ADDRESS(ES)

SE Laser Physics
Birzhevaya line 14
St. Petersburg 199034
Russia

8. PERFORMING ORGANIZATION REPORT NUMBER

N/A

9. SPONSORING/MONITORING AGENCY NAME(S) AND ADDRESS(ES)

EOARD
PSC 802 BOX 14
FPO 09499-0200

10. SPONSORING/MONITORING AGENCY REPORT NUMBER

SPC 99-4053

11. SUPPLEMENTARY NOTES

12a. DISTRIBUTION/AVAILABILITY STATEMENT

Approved for public release; distribution is unlimited.

12b. DISTRIBUTION CODE

A

13. ABSTRACT (Maximum 200 words)

This report results from a contract tasking SE Laser Physics as follows: The contractor will investigate holographic correction of the image of an extended object observed through the telescope with a thin-film elastic primary mirror having a dynamic diffractive optical element on its surface.

14. SUBJECT TERMS

EOARD, Aberration correction, Astronomy, Deep space imaging, Diffractive optical elements, Imaging telescopes, Non-linear Optical Materials , Optical aberrations

15. NUMBER OF PAGES

16. PRICE CODE

N/A

17. SECURITY CLASSIFICATION OF REPORT	18. SECURITY CLASSIFICATION OF THIS PAGE	19, SECURITY CLASSIFICATION OF ABSTRACT	20. LIMITATION OF ABSTRACT
UNCLASSIFIED	UNCLASSIFIED	UNCLASSIFIED	UL

List of authors:

M.P. Bogdanov
O.G. Bol'shukhin
S.A. Dimakov - principal investigator
A.V.Gorlanov
S.I Kliment'ev
I.V. Korableva
I.B. Orlova
V.E. Sherstobitov - scientific leader
N.A. Sventsitskaya
D.I. Zhuk

Technical group:

A.M. Kokushkin

Contents

(*) Footnote: The dual numbering of the items in this section is related to that this section contains the results concerning the two corresponding items of the Contract.

Introduction

With ever-growing number of publications related to studies of properties of the imaging telescopes with nonlinear correction of image distortions, these telescopes appear to be more and more customary. In recent years this rapidly developing application of the nonlinear optics is the subject of special conferences, for instance, such as conference "Laser Optics 98" (St. Petersburg) or SPIE Meetings (San Diego 1998, Baltimore 1998, Denver 1999).

The number of papers on this subject amounts now to several tens. Therefore within the scope of this report we will not discuss the optical scheme of such a telescope having in mind it to be known. Note, however, that in the telescopes with nonlinear optical correction considered in the scientific literature there usually exists some optical element enabling a non-reciprocal bypass of the mirror which distortions are to be compensated. As such an element either a conventional beam splitter (in so called "bypass schemes") or a diffractive optical element (DOE) on the primary or even secondary mirror surface (TENOCOM scheme) may be used.

The mentioned telescope versions are characterized by high correction fidelity being different for various distortions of the primary. The correction fidelity depends on a variety of factors the main of which are both wavelength inequality between the recording and the object beams and difference of local angles of incidence at the primary mirror for the mentioned beams.

The latter factor of deterioration of correction fidelity might be substantially minimized in the telescope version with a DOE on the primary mirror. (See Section 2 of the Final Report on Contract F61775-98-WE089 (project SPC-98-4065) "Nonlinear-optical correction of aberrations in imaging telescopes based on a diffraction structure on the primary mirror".) This effect is achieved by a proper choice of the DOE so that the beam from a special point source pertaining to the telescope is diffracted by the DOE and thus produces the beam recording the

corrector. This beam has its wave-front curvature being close or even equal to that of the beam coming from a remote object.

We assume DOE on the primary to be of a static or dynamic type. We consider these types of DOE and compare their features in Section 1 of this report.

Note that the dynamic hologram concept here as well as that elsewhere now is wider as compared to one used earlier. Originally this term was used to signify that the beams diffracted by the hologram (secondary beams) were also involved in the recording process together with the primary recording beams. At present "dynamic" hologram means a "reversible" one (it can be erased and a new pattern recorded) in conditions of changing characteristics of the recording process (e.g. variation of the object-beam wave front), in addition to the former meaning.

Section 2 presents the data available in literature on the nonlinear optical materials promising for recording dynamic DOE. First of all the requirements to nonlinear media suitable for recording dynamic holograms on membrane mirrors are considered. It is caused by the specific character of the task, since, e.g., not every of known holographic media can behave correctly being deposited on a membrane material.

Then a brief survey is given of materials (available in the scientific literature) which could meet the requirements of the task under consideration. It should be noted that the best choice of the media needed might be done basing on characteristics of the membrane primary to be coated with DOE, and also on the design features of the optical system where this mirror will be employed. Without knowing specific parameters of the mirror we could not select the optimal holographic medium for our task. So we considered the media being studied most actively now and showing acceptable physical technical characteristics.

We presented also a brief description of materials to be the potential candidates for our experiments under the current Contract. Here we confined ourselves to concerning with the available media which though having not best characteristics, enable achieving the desired result, namely, the demonstration of the record/read-out cycle of holograms on the membrane surface.

Fabrication of small-dimension experimental samples for the experiments on recording/read out of DOE on elastic substrates simulating the membrane PM is described in Section 3.

Section 4 describes optical parameters of the samples fabricated (based on thermoplastic and bacteriorodopsin).

The theoretical and experimental studies of static DOE, most interesting from the stand point of practice, on membrane PMs are presented in section 6.

The report is completed by a comparative analysis of applicability of dynamic and static DOE on large aperture membrane mirror. In this comparison which might be effective for concrete samples, we confined ourselves to finding out in general their advantages and disadvantages.

Section 1. Analysis of conditions of adequate getting information on membrane mirror distortions when using DOE on the mirror surface

One of the prospective schemes for telescopes with nonlinear optical correction for PM distortions is the scheme comprising DOE on the PM surface. The advantages and disadvantages of this scheme were thoroughly considered in the previous [1] report. They were also compared with advantages and disadvantages of the 'by-pass' and TENOCOM versions. In this work we have paid special attention to the operation peculiarities of this scheme related to employment of the DOE on the mirror surface. Below we evaluate operation gains of both static and dynamic DOEs. However first of all we consider the general aspects concerning the additional distortions inherent in DOE as well as some special technical problems one encounters with this scheme. Throughout here we assume this element to be recorded by light (see [1]). DOE applied on PM surface serves to pass information on mirror's distortions to the nonlinear corrector involved in the telescope system.

Let us firstly consider the conception of the 'ideal' scheme for recording DOE on the PM surface and reading out its distortions (Fig.1.1). One of the beams is a spherical wave emitted by a point source O_r placed at a some distance from the mirror. The other beam has a plane wave front and is formed either by a point-like source in the infinity or by a point source at a finite distance from the mirror O_o. In the last case the spherical wave front can be transformed into the plane one with the use of a beam-forming system. The intensity distribution of the two interfering beams is converted into the holographic grating of the refraction index distribution in the nonlinear material applied on the mirror. When recording the nonlinear corrector in the telescopic system we use the beam of an auxiliary laser sited at the same point O_r. As is well known in holography this beam diffracted on the hologram acquires in the minus-first diffraction order the plane wave front like that of the other beam. It hits the mirror surface and, having been reflected, passes through DOE (in zero diffraction order) and converges into PM focus. This very beam bearing information on mirror distortions is employed to record the mentioned above nonlinear corrector in the telescopic system (e.g., an imaging one).

In the case of object observation, the beam with a plane wave front (from a remote object) passes through the holographic grating and hits upon the mirror surface (zero diffraction order). Then reflected by the mirror, it (passing the grating as the zero-diffraction-order beam) converges in the mirror focus. Thus it is fully identical to the auxiliary-laser focusing beam earlier recorded the nonlinear corrector. It is due to this identity the high-fidelity holographic correction for the image distortions caused by the surface deformations of the PM can be actualized. However, realization of this correction scheme being 'ideal' from the standpoint of maximum compensation fidelity seems to be virtually impossible. This is related with necessity of employment of a non-aberrated large-scale optics for recording DOE. Here we encounter that very problem of a high-quality large-aperture mirror that is the subject of this Contract.

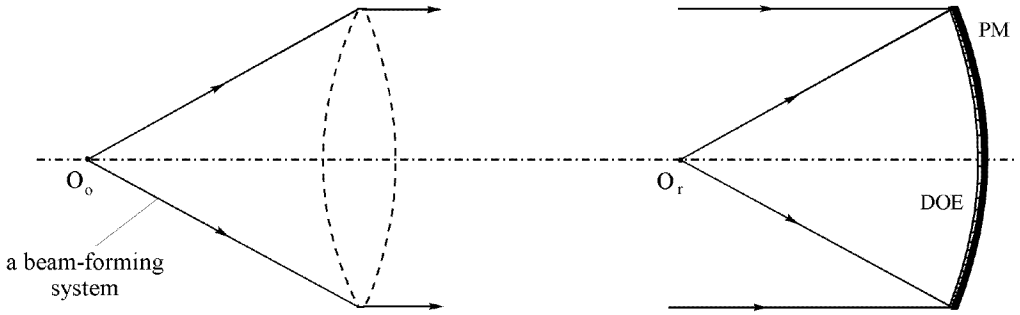

Fig.1.1. "Ideal" conception of recording DOE with the use of the wave from a point source O_r and the plane wave.

Thus we have to exclude a large-scale beam-forming optics while recording DOE. The idea is to record DOE with two beams of point-like sources placed at some finite distances from the PM (Fig.1.2). The holographic phase grating on the mirror surface recorded by these two interfering beams is given as

$$\varphi_g(X) = \frac{2\pi}{\lambda_{rec}} (\psi_o(X) - (\psi_r(X)) , \tag{1}$$

where

$$\psi_{o,r}(X) = \sqrt{X^2 + (Z_{0,r} - \delta(X))^2} - Z_{o,r} . \tag{2}$$

Here $Z_{o,r}$ notes the distances of the point sources O_o and O_r (see Fig.1.2) from the mirror vertex, and $\delta(X)$ the surface shape of the mirror which looks like

$$2\rho\delta(X) = X^2 + \varepsilon\delta(X), \tag{3}$$

where ρ is the curvature radius at the mirror vertex, and ε eccentricity function. Here $\varepsilon = 0$ corresponds to a parabolic shape of the mirror surface.

Reading out the mirror distortions is implemented with the beam of an auxiliary source placed in point O_c so that, being reflected from the mirror with DOE, the beam converges in the mirror focus. As was mentioned above this beam must have parameters identical to those of the beam coming from a point-like source in the infinity. We neglect here the distortions acquired by the object beam on its propagation path. Thus we come to the problem of determination and reduction of an aberration magnitude in the beam reflected from the mirror with DOE. To control the characteristics of this beam we can choose the sites of the sources used for recording DOE, namely the distances Z_o and Z_r, as well as the distance Z_c of the source for reading out the mirror distortions. We can also choose the wavelength of recording and reading out light.

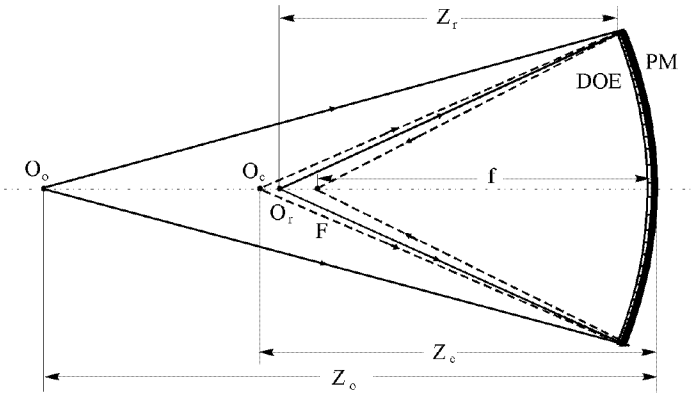

Fig.1.2. Recording DOE on the PM surface with the beams of point sources O_r and O_o and reading out PM distortions with the beam of a point source O_c.

Let us consider how the aberration of the beam reflected from the mirror with DOE arises. The beam coming from the point O_c has its phase distribution on the mirror surface written as

$$\varphi_{inc} = \varphi_c + \varphi_g, \tag{4}$$

where

$$\varphi_c = \frac{2\pi}{\lambda_{read}} \sqrt{X^2 + (Z_c - \delta(X))^2} - Z_c. \tag{5}$$

Then the phase distribution of the reflected beam on the mirror surface is

$$\varphi_{refl} = - \varphi_c - \varphi_g. \tag{6}$$

The aberration of this reflected beam as compared with that of the 'ideal' beam converging in the mirror focus is determined as the phase difference

$$\Delta W = - \frac{2\pi}{\lambda_{read}} (\psi_c(X) + \mu(\psi_o(X) - \psi_r(X)) + \psi_F(X)), \tag{7}$$

where

$$\psi_F(X) = \sqrt{X^2 + (f - \delta(X))^2} - f, \tag{8}$$

where f is the mirror focal length, and

$$\mu = \frac{\lambda_{read}}{\lambda_{rec}}. \tag{9}$$

In the third-order-aberration approximation the function $\psi_i(X)$ (i notes any of the indexes o, r or F) takes the form

$$\psi_i(X) \cong \frac{1}{2Z_i}\left(1 - \frac{Z_i}{\rho}\right)X^2 - \frac{1}{8}\left(\frac{1}{Z_i^3} - \frac{2}{\rho z_i^2} + \frac{\varepsilon}{\rho^3}\right)X^4. \tag{10}$$

This approximation is often used for calculation of optical systems. The higher-order approximations or even the exact aberration formulas are only employed when designing the concrete optical system. However they are virtually unexpressed in a simple analytic form and appear to be time consuming ones for calculations of system parameters.

Substitution (10) in (7) gives the aberration of the reflected from the mirror with DOE beam as:

$$\Delta W = \Delta W_{def} + \Delta W_{sph} + \Delta W_{high}, \tag{11}$$

where ΔW_{def} and ΔW_{sph} are the defocusing and spherical aberrations determined as

$$\Delta W_{def} = -\frac{\pi}{\lambda_{read}}\left[\frac{1}{Z_c} + \mu\left(\frac{1}{Z_0} - \frac{1}{Z_r}\right)\right]X^2, \tag{12}$$

$$\Delta W_{sph} = -\frac{\pi}{\lambda_{read}}\left[\frac{1}{Z_c^3} - \frac{1}{fZ_c^2} + \mu\left(\frac{1}{Z_o^3} - \frac{1}{Z_r^3} - \frac{1}{f}\left(\frac{1}{Z_o^2} - \frac{1}{Z_r^2}\right)\right)\right]\frac{X^4}{8}, \tag{13}$$

ΔW_{high} notes the higher-order aberrations, (we assume here ε=0).

The parameters of the optical system for recording DOE and reading out mirror distortions may be chosen from the conditions the defocusing and spherical aberrations to be zero in magnitude. The focusing condition for the beam reflected from the mirror with DOE $\Delta W_{def}=0$ leads to the following relation between the distances of the sources O_o, O_r, and O_c from the mirror:

$$\frac{1}{Z_o}-\frac{1}{Z_r}+\frac{1}{\mu Z_c}=0. \tag{14}$$

The other condition $\Delta W_{sph}=0$ leads to the expressions for the distances Z_o and Z_r via Z_c and μ:

$$\frac{1}{O}=\frac{1}{2}\left[\frac{2}{3}-\frac{1}{\mu C}+\frac{1}{\sqrt{3}}\sqrt{\left(\frac{4}{3}+\frac{4}{C^2}-\frac{4}{C}-\frac{1}{(\mu C)^2}\right)}\right],$$

$$\frac{1}{R}=\frac{1}{2}\left[\frac{2}{3}+\frac{1}{\mu C}+\frac{1}{\sqrt{3}}\sqrt{\left(\frac{4}{3}+\frac{4}{C^2}-\frac{4}{C}-\frac{1}{(\mu C)^2}\right)}\right], \tag{15}$$

where

$$O=\frac{Z_o}{f}, \qquad R=\frac{Z_r}{f}, \qquad ?=\frac{Z_c}{f}. \tag{16}$$

The obtained equations (14) and (15) are the basis for the choice of the system optimization ways aimed at lowering the total aberration of the beam reflected from the mirror with DOE.

Fig.1.3 shows dependence of O and R on μ at $C=1$. As is seen, larger μ allows one to place the sources O_o and O_r recording DOE closer to one another, the nearest to the mirror source O_r being sited farther and the remote one O_o closer to the mirror. Thus, the total length of the optical system can be reduced. For instance, at μ=2.2 the source O_r is at the distance ~1.15f from the mirror and the source O_o approximately at the distance ~2.42f whereas at μ=1.2 these distances are Z_r≈1.02f and Z_o≈6.78f.

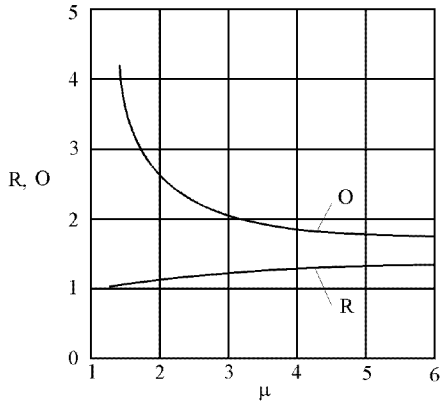

Fig.1.3. Dependence of the relative distances R and O on μ at C = 1.

Fig.1.4 shows the high-order-aberration distribution (ΔW_{def} and ΔW_{sph} being zero) across the beam section (on the mirror surface) at the relative aperture $A=D/f=1$ and $\mu=1.2$. As is seen, the high-order total aberration increases to the mirror edge. It has the more magnitude the more the relative aperture of the mirror. This aberration also increases with growing μ. Thus effects of C and μ on the residual aberration magnitude (comprising only high-order aberrations) seem to be very important from the standpoint of optimal correction for PM distortions in the telescope system. In all the calculations in this section we used $\lambda_{read}=1\mu m$ and $f=5m$.

Fig.1.5 shows dependence of the maximum (corresponding to $X=D/2$) total high-order aberration on C at $A=1$ and $\mu=1.2$ and 2.2. As is seen in the figure, C-function of the total aberration has its apparent maximum which absolute magnitude increases with growing μ. The related sites of the sources recording DOE and reading out the mirror distortions are also in dependence on μ. Table 1.1 examples positions of the sources O_o, O_r, and O_c corresponding to the minimum total high-order aberration (at zero defocusing and spherical aberrations).

Table 1.1.

μ	Z_r/f	Z_o/f	Z_c/f	$\Delta W_{resid}/2\pi$
1.2	1.165	7.00	1.165	-35.737
1.8	1.448	3.25	1.450	-111.164
2.2	1.548	2.83	1.550	-128.369

Note also that the position of the nearest to the mirror source recording DOE (O_r) is close to that of the reading-out beam source (O_c). The calculations showed that for a mean-size relative aperture (A~0.4) the minimal relative high-order aberration at the mirror edge amounts to about a half whereas for a large aperture (A=1) it exceeds a hundred.

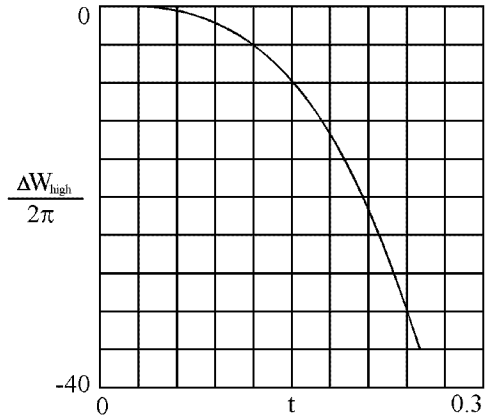

Fig.1.4. High-order-aberration distribution in the beam cross-section.

High-order aberrations can be compensated with a special phase-compensating element based on a hologram (or traditional optics) technique. It might be like a phase screen having its profile corresponding, for example, to the aberration of the next order in reference to the spherical aberration (that is $\sim X^6$) with the opposite sign.

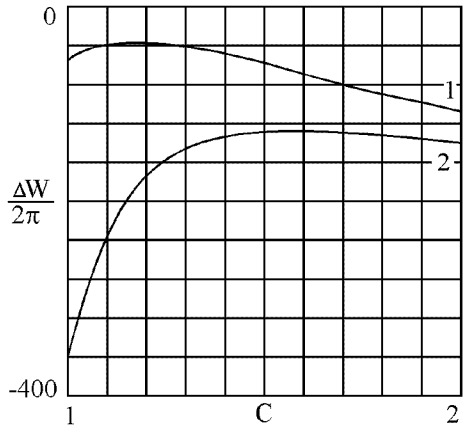

Fig.1.5. Total high-order aberration versus C,
A=1, μ=1.2 (**1**); μ=2.2 (**2**).

Fig.1.6 presents the residual aberration in the beam section (on the mirror surface) $\Delta W_{resid}(t)$ after phase-correction with the use of the phase element $Q(t)$. This residual aberration is determined as the difference

$$\Delta W_{resid}(t) = \Delta W_{high}(t) - Q(t), \qquad (17)$$

where $Q(t)=-b\chi t^3$ and $t=(X/f)^2$.

With the proper choice of the factor χ (depending on both A and μ) the residual aberration may be obtained of a sufficiently small amount.

Table 1.2. illustrates the χ - factor magnitude depending on μ at $A=1$.

Table 1.2.

Parameters	μ=1.2	μ=2.2
χ	$4.58 \cdot 10^{-4}$	$16.425 \cdot 10^{-4}$
$\Delta W_{resid}(t)/2\pi$	<±0.1	<±0.1

The phase-compensating elements of this kind may be placed in the reflected beam under consideration and/or in the beams recording DOE. In the last case the phase-profile magnitude (χ) might be μ times less. The sign of the phase profile depends on that in which of the beams this element is put. Thus we have considered the aberrations related only to the record/read-out optical scheme assuming the mirror surface to be an ideal parabola.

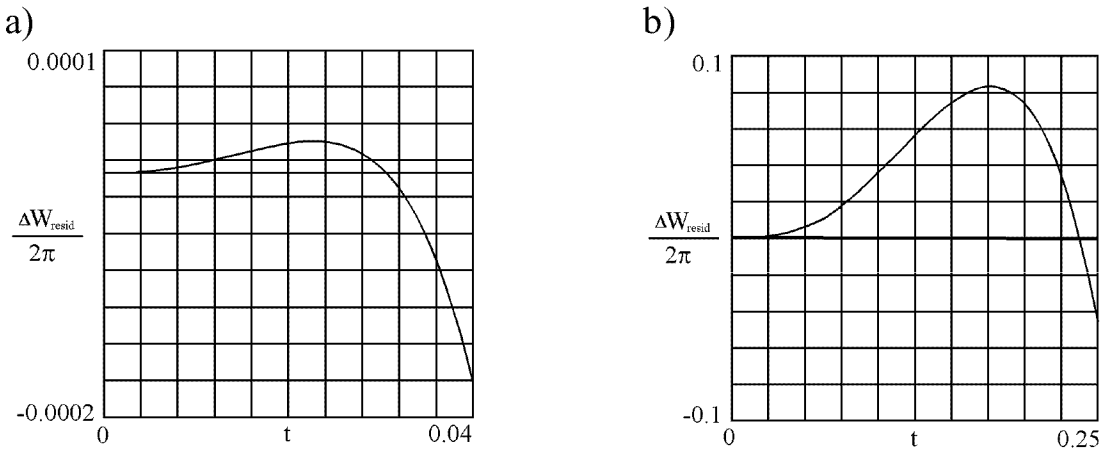

Fig.1.6. Residual aberration after phase correction with the use of a special phase-compensating element μ=2.2, a) A=0.4, b) A=1.

Now we are going to take into account the aberrations related to deformations of the mirror when both recording DOE and observing an object. We are also going to compare two versions of DOE, namely static DOE and dynamic one. By a dynamic DOE is meant the element to be recorded and read out during the periods less than the characteristic times mirror deformations so that its phase structure follows the surface shape of the mirror. It is well known in holography that each of two beams recording a hologram diffracts on it in the direction of the other beam independently on phase distortions of their wave fronts. However it is not true in the case of another beam diffracted on the hologram. This very situation we have when recording the dynamic DOE on the mirror surface and reading out the mirror distortions through it with the beams from the different sources. In this case the hologram brings into the diffracted

beam its own impress. Concerning the static DOE considered below we mean it to be 'ideal' in its phase structure and unchanged with mirror deformations. In particular the static DOE may be actualized on an additional film surface like that in [2] separated from the mirror.

Fig.1.7 shows the deformed mirror surface with DOE applied on it. With the use of formulas (1)-(8) in which we confined ourselves to the values of the first degree of a small amount h that is valid for $h/f<<1$, we write the total aberration of the beam reflected by the mirror with dynamic DOE in the form

$$\Delta W_{total} = \Delta W + \frac{2\pi}{\lambda_{read}}\left(\frac{h}{1-\frac{t}{8}}\right)\left\{\frac{\left(C-\frac{t}{4}\right)}{\sqrt{\left(C-\frac{t}{4}\right)^2+t}} + \frac{\mu\left(O-\frac{t}{4}\right)}{\sqrt{\left(O-\frac{t}{4}\right)^2+t}} - \frac{\mu\left(R-\frac{t}{4}\right)}{\sqrt{\left(R-\frac{t}{4}\right)^2+t}} + \frac{\left(1-\frac{t}{4}\right)}{\left(1+\frac{t}{4}\right)}\right\}, \qquad (18)$$

where ΔW is the beam aberration expressed by (7), h local deformation of the mirror surface along its normal, $t=(X/f)^2$. For simplicity we assume now that this surface is a parabolic one so that $\varepsilon=0$ and determine $\delta(X)$ in (2), (5), (8) by the following approximate equation

$$\delta(X) = \frac{tf}{4} - \frac{h}{\left(1-\frac{t}{8}\right)}, \qquad (19)$$

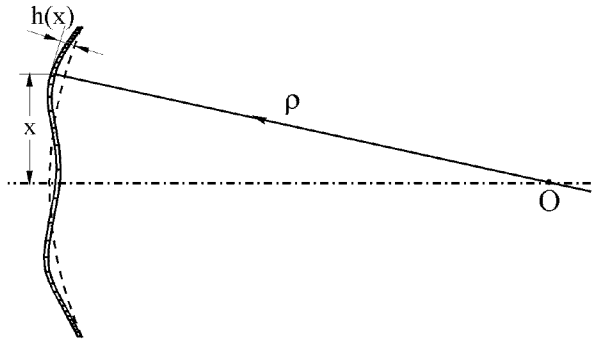

Fig.1.7. Deformed mirror with DOE on its surface
h-local deformation of the mirror.

As was said above, aberration ΔW (the first term in (18)) related to the record/read-out optical geometry might be canceled out with correct selection of the scheme parameters and employment of the special phase-compensating elements. The second addendum in (18) is the aberration related to deformations of the mirror surface. It is in direct proportion to the local mirror deformation h. The proportionality factor is determined by the parameters of the system for recording DOE and reading out mirror distortions. Compensation for aberrations

of the deformed PM in the telescope system comprising the image-distortion nonlinear corrector is based on adequacy of reading out mirror deformations in the channel for recording the corrector and in the observation channel. This means that the difference of the aberrations in the object beam reflected from the mirror and in the minus-first-diffraction-order beam of the point source O_c must be close to zero in magnitude. The extent of residual aberration diminishing determines the telescope image-correction fidelity.

Therefore let us compare ΔW_{total} (18) with the aberration ΔW_{obj} the object beam acquires being reflected by PM. In the case of observation of an object in the infinityΔW_{obj} is given by

$$\Delta W_{obj} = - \frac{2\pi}{\lambda_{read}} \left(-\frac{tf}{4} + \frac{h}{1-\frac{t}{8}} + W_F(t) \right). \qquad (20)$$

Taking into account (8) and (19) we obtain

$$\Delta W_{obj} = \frac{2\pi}{\lambda_{read}} h \left[\left(1 - \frac{t}{8} \right) \right]^{-1} \left[\frac{h}{1-\frac{t}{8}} \cdot \frac{2}{1+\frac{t}{4}} \right], \qquad (21)$$

Thus the residual aberration in the case of object observation via the deformed PM is

$$\Delta W_{resid} = \Delta W_{obj} - (\Delta W_{tot} - \Delta W), \qquad (22)$$

Fig.1.8 shows the relative residual aberration $\Delta W_{resid}\lambda_{read}/2\pi h$ at $A=1$ and $\mu=1.8$ and 2.2. The calculations showed that the residual aberration at $\mu=1.8$ in the system comprising the phase-compensating element may be brought down to 0.1 at local deformations of the mirror of several tens wavelengths for $A=0.4$ or several units of λ for $A=1$.

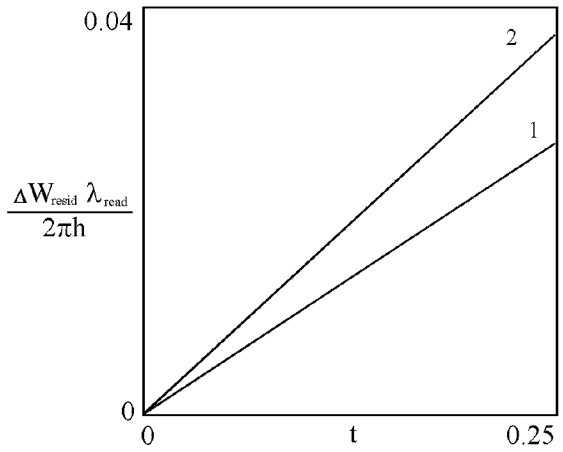

Fig.1.8. Relative residual aberration in the observation channel (with nonlinear image corrector) Dynamic DOE
1-μ=1.8, **2**-μ=2.2.

For the comparison let us consider the static DOE applied on the mirror surface. We assume now that the DOE is recorded on the 'ideal' mirror's surface and its phase structure does not change with mirror deformations. In this case the residual aberration differs from that in the case of the dynamic DOE. This is related to that the static DOE phase structure being independent on the deformed mirror shape brings an additional phase error in the recording corrector channel as compared with that in the observation channel. This additional aberration ΔW_{add} is written as

$$\Delta W_{add} = -\frac{2\pi h}{\lambda_{read}\left(1-\frac{t}{8}\right)}\left\{\frac{O-\frac{t}{4}}{\sqrt{\left(O-\frac{t}{4}\right)^2+t}}-\frac{R-\frac{t}{4}}{\sqrt{\left(R-\frac{t}{4}\right)^2+t}}\right\}. \qquad (23)$$

The estimates similar those above for dynamic DOE show that static DOE reduces the allowable mirror distortions in magnitude at the same μ approximately two times for A=0.4 and three times for A=1 as compared to those in the case of dynamic DOE.

Using formula (23), we assume the lines of the DOE diffraction structure to change their positions only along the optical axis of the PM. In reality the mirror's deformations result in some shifts of the diffraction structure lines in the transverse directions too. Thus the static DOE restricts allowable deformations of the mirror to a greater extent. The related estimates similar those in [3] may be done basing upon that the shifts must be small as compared with the spatial period of the considered diffraction structure.

It should be noted that errors in positions of the used light sources along the PM optical axis lead to defocusing and spherical aberrations in the beam recording the nonlinear corrector of the telescopic system. So let us estimate the allowable displacements of the sources recording the DOE and the source of the beam reading out mirror's distortions. For this we differentiate functions ΔW_{def} and ΔW_{sph} (12), (13) with respect to Z_o, Z_r, and Z_c and take the first derivatives in the points corresponding to zero both defocusing and spherical aberrations, and to the minimum total high aberration. We obtain the allowable displacements related to the defocusing aberration in the form

$$\begin{aligned} \left|dZ_r^{(d)}\right| &= 8\cdot\delta W_{def}\cdot\left(\frac{R}{A}\right)^2\cdot\frac{\lambda_{read}}{\mu} \\ \left|dZ_o^{(d)}\right| &= 8\cdot\delta W_{def}\cdot\left(\frac{O}{A}\right)^2\cdot\frac{\lambda_{read}}{\mu} \\ \left|dZ_c^{(d)}\right| &= 8\cdot\delta W_{def}\cdot\left(\frac{C}{A}\right)^2\cdot\frac{\lambda_{read}}{\mu}\quad , \end{aligned} \tag{24}$$

and to the spherical aderration in the form

$$\begin{aligned} \left|dZ_r^{(s)}\right| &= \frac{64}{3}\cdot\delta W_{sph}\cdot\frac{\lambda_{read}}{\left(1-\frac{2}{3}R\right)}\cdot\frac{2}{\mu}\cdot\left(\frac{R}{A}\right)^4 \\ \left|dZ_o^{(s)}\right| &= \frac{64}{3}\cdot\delta W_{sph}\cdot\frac{\lambda_{read}}{\left(1-\frac{2}{3}O\right)}\cdot\frac{2}{\mu}\cdot\left(\frac{O}{A}\right)^4 \\ \left|dZ_c^{(s)}\right| &= \frac{64}{3}\cdot\delta W_{sph}\cdot\frac{\lambda_{read}}{\left(1-\frac{2}{3}C\right)}\cdot\frac{2}{\mu}\cdot\left(\frac{C}{A}\right)^4\quad , \end{aligned} \tag{25}$$

where δW_{def} and δW_{sph} are the allowable defocusing and spherical aberrations for an edge ray.

It results from (23), (24) that the allowable displacements related to spherical aberrations prevail more than an order over ones related to defocusing aberrations. The accuracy requirements for positioning the source O_r are much more strict as compared with those for O_o. For example, the allowable displacements of the source O_r amount for the accepted $\delta W_{def}=0.1$ to units of a

micrometer at A=0.4, and fractions of a micrometer at $A=1$ and μ ranging from 1.2 to 2.2. So the source positions are taken to provide the spherical aberration to be of an allowable magnitude. Then the source O_c is shifted to provide the defocusing aberration close to zero in magnitude. It is possible because displacements of the source O_c are allowable in a rather wide range.

Now we dwell briefly on resolution capacity of the considered DOEs. The DOE local-spatial-frequency distribution over the mirror surface is given by

$$\nu(x) = \frac{1}{2?\lambda_{read}} \cdot \left\{ -2\frac{X}{f} + \left(\frac{X}{f}\right)^3 \left(\frac{1}{C^2} - \frac{1}{C}\right) \right\} \qquad (26)$$

Fig.1.9 shows distribution over the mirror's surface of the DOE local spatial frequencies for the case of $A=1$, and $\mu=1.2$ and 2.2. As is seen, $\nu(X)$ is in inverse proportion to λ_{read}. So increase of the wavelength ratio μ and hence reduction of λ_{rec} (all other things being the same) leads to reduction of the maximum local frequency of DOE.

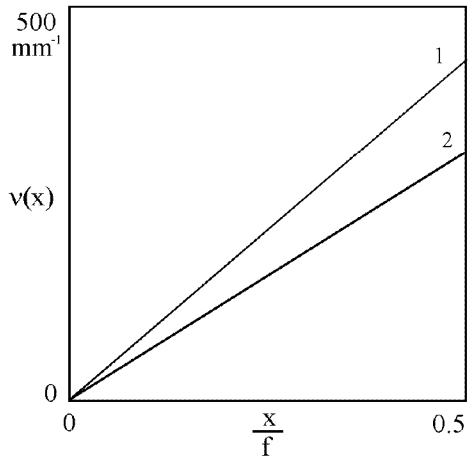

Fig.1.9. DOE spatial frequency distribution along mirror's radius A=1, μ=1.2 (**1**), μ=2.2 (**2**).

In conclusion it should be noted that the considered geometry for recording DOE/reading out mirror distortions allows one to decrease the total length of the telescope system, but offers its own aberration undesired from the standpoint of the telescope's nonlinear corrector. These two tendencies conflict with one another. So design of a telescope with DOE on its primary requires a trade-off between the system length and aberration to be compensated with the use of special phase-compensating elements.

Section 2. Nonlinear media suitable for recording a dynamic DOE

2.1. Requirements to nonlinear media suitable for recording dynamic holograms on membrane mirrors

All requirements to holographic materials may be classified as common and additional ones. The common requirements are those typical for holographic materials. They involve:

- the necessary working spectral range;
- high sensitivity to the recording light;
- a broad range of intensity of the recording light;
- the required diffraction efficiency;
- minimum losses of the read-out light (no scaterring at random inhomogeneities in the medium, low losses for absorption, and necessary reflection for reflecting relief holograms);
- high resolution capability.

The concrete values of characteristics of the mentioned materials are to be naturally dependent on the task being solved.

As the additional requirements are considered those related to specific usage of a nonlinear holographic material applied to the surface of the membrane mirror being the primary of the telescopic system with nonlinear optical correction of dynamic distortions.

Let us consider the essence of these requirements:

- The important parameters of the holographic process of compensation for the membrane-mirror dynamic distortions are reversibility of the recording/read-

out cycle and its duration in a pulse-repetition operation mode. In the case of the CW mode the substantial parameter is the response time of the material. The requirements to the temporal parameters consist in that the characteristic times of the material must be essentially shorter as compared with those of dynamic distortions.

It is known that in telescopic systems the dynamic distortions are possible with characteristic times being in the range of several seconds to milliseconds. Slowly changing distortions (with frequencies up to several Hz) are conditioned by thermal, gravitational and inertial disturbances, and fast ones are, as a rule, associated with vibration and acoustic perturbations. Therefore even the nonlinear media with response of about seconds are of interest since they enable one to compensate for static as well as slow dynamic distortions usually being of rather large magnitude.

- In the case of a pulse-repetition operation mode an additional requirement to the nonlinear medium is that of minimum average specific power (along with high sensitivity) of the laser beams recording the hologram.

This requirement is very important. The reason is that, firstly, it determines the required power of the laser source, and consequently, its tolerable mass, dimensions and energy consumption. These are especial for the large-size membrane primary mirror of a telescopic system. Secondly, it determines the thermal regime of the membrane mirror's surface and thus its temperature.

- The working spectral range of the nonlinear material must provide effective both recording/read-out of a hologram and observation of an object. Note here that, as it results from the analysis conducted earlier (at the first stage of the work under this Contract), recording of holograms can be executed with shorter wavelengths as compared to those for both read-out of holograms and observation of objects.
- The requirements to diffraction efficiency of the hologram recorded on the membrane mirror appear to be conflicting for the two operation stages of the correction system. On the one hand, at the read-out stage the maximum diffraction efficiency is desired. On the other, high diffraction efficiency results in abatement of the object-beam intensity at the observation stage. To provide high performance of the system a tradeoff is needed between the mentioned requirements. This must enable one to employ the nonlinear media with not high diffraction efficiency (less than 1%) and at the same time sufficiently easy compensate for lack of their diffraction efficiency by power increase of the beam bearing the distortions.
- The requirements to resolution capability of the materials for the primary-mirror application are of some specific nature. This is associated with the character of the holograms employed. To a first approximation these holograms are akin to Fresnel's zone plates. Indeed, the hologram consists of concentric rings coaxial in respect to the mirror's center. In accordance with the known Fresnel's formula, the local spatial frequency of the rings increases

toward the membrane's edge. (Thus, simple estimates for the mirror with its relative aperture D/F=1:2 and 1m in diameter showed that the spatial frequency for λ=0.5μm amounts to about 480 mm^{-1} at the hologram's edge).

Some materials suitable for recording these holograms show low potentials for recording small spatial frequencies (e.g., photo-thermo-plastics work effectively only at spatial frequencies above 10-15 mm^{-1}). However they could be used for operation on the primary mirror since its central zone being disadvantageous for them is not usually employed in many optical systems. Note that the required maximal spatial frequency of the hologram recorded on high-relative-aperture primary mirrors in the visible spectrum does not exceed 2500 mm^{-1}.

- The essential requirement for operation on large-aperture membrane mirrors is that of good adhesion of the nonlinear material to the substrate. This will prevent slacking of the material in the conditions of variable curvature of the membrane surface during operation and also in the case of mounting and transporting of the mirror. The nonlinear material is required to be sufficiently elastic to exclude its possible influence on the mechanical features of the membrane that may be metallic as well as polymeric. Note that some materials may be directly implanted into the membrane being a polymer film having a specular coating on its back surface. In this case a constant optical thickness of the membrane must be provided.
- In some cases one should take into account the requirements to the parameters of the environment during operation of the mirror-surface dynamic hologram. Many of nonlinear materials are sensitive about their working temperature and its distribution over the mirror's surface. Some of them require gas medium around for their success operation, some allow no both scattered or local irradiation from any light sources. Therefore all the materials for recording holograms on the membrane mirrors designed for operation in space conditions must meet some additional requirements.
- Special requirements arise at the stage of deposition of the holographic material on the membrane mirror's surface. The required large area as well as necessity of homogeneity and thickness uniformity of the coating layer result in high technological requirements which can be met not for every of the nonlinear materials. For instance, composites of thin semiconductor layers and liquid crystals, which are effective in spatial light modulators (SLM), do not meet this criterion. It discomforts one to employ these materials for recording holograms on the membrane mirrors.

Considering nonlinear materials that could be promising for registration of static and dynamic holograms on membrane surfaces, we took into account first of all the basic, most general requirements. We mean that, having a most promising material, we could adapt it to a concrete research task in the course of our further work.

2.2. Nonlinear media suitable for recording a dynamic DOE

A lot of nonlinear media suitable for recording phase holograms are known presently. These media are usually classified in two groups. One group comprises materials in which changes of the refractive index occur under exposure to a light wave as such (e.g. due to non-elastic photon scattering in the Kerr effect). In the materials of the other group changes of the refractive index arise due to various nonlinear processes resulting from absorption of light energy in the medium. Thermal nonlinear processes, generation of non-equilibrium charge carriers in semiconductors, photo-refractive and electro-optical processes, and some others may be the examples of processes of such sort. The materials related to the first mentioned group are characterized by a high speed of the recording and relaxation processes. However their efficiency appears to be very low due to a short lifetime of the light-induced gratings. Therefore the high power laser sources are required for recording holograms in these materials. The holographic-application area of the materials of the second group appears to be wider as compared to those related to the first one.

2.3. Photorefractive crystals

The photorefractive mechanism of recording is one of most traditional in holography and in particular in dynamic holography. It was observed and studied with a variety of inorganic crystals such as LiNbO3, BaTiO3, SBN, BSO and some others.

Earlier in our experimental studies of peculiarities of compensation for distortions in a telescopic imaging system, we employed photorefractive crystals BSO and SBN as media for recording of the nonlinear optical corrector. These media proved to be good, showing high both diffraction efficiency and sensitivity, fast response, and a low level of noises. Using these crystals we could demonstrate high effectiveness of dynamic-distortion compensation while observing objects through a model telescope with its solid, segmented, or elastic primary mirror. However these media appear to be unacceptable for recording DOE on membrane mirrors.

Fabrication and exploitation of an elastic mirror with a thin layer of a crystalline photorefractive material on its surface seems to be rather problematic. The reason is that, firstly, no technology is available for growing these crystals of sufficiently large dimensions and required high optical quality. Secondly, such a crystalline layer proves to be rigid and fragile and shows low adhesion with an elastic film substrate. And thirdly, reduction of thickness of a nonlinear medium results in unavoidable lowering of hologram diffraction efficiency.

Thus restrictions characteristic of these crystals make them noncompetitive in regard to novel, more prospective polymer photorefractive materials (see, e.g., [4]).

2.4. Organic photosensitive materials

Organic photo-sensitive materials, in particular, photopolymers appear now to be more and more forehand in various holographic applications due to their high sensitivity and sufficiently fast response. Nonlinear optical features of most of polymer holographic materials are determined by dipolar chromophores introduced into a polymer either via doping or through covalent bonds with polymer's molecules. Introduction of photochromic molecules in organic materials results in development of photorefractive or macro-photo-sensitive systems with light-controlled properties. Due to flexibility of structural and chemical modifications, these materials have more potentials for optimizing their features by variations of their composites or experimental conditions as compared to those of traditional materials for holography. It is important to note as well easiness and comparatively low cost of fabrication of thin polymer films. This allows fabricating of samples of both large dimension and various forms, having optical characteristics required for a concrete application.

Photopolymers are usually employed for recording volume phase holograms which present either a spatial distribution of refraction index changes or a surface relief of the material. They are mainly used for recording of transmission holograms. Publications on recording of reflection holograms in photopolymers ($OmniDex^{R}_{706}$) are met utterly seldom. Recording mechanisms in polymers based on both thermal and photon processes are substantially more various than those in inorganic materials. Here occur the traditional for inorganic media mechanisms such as the photorefraction and electro-optic effects and also mechanisms inherent in organic compounds only such as various reactions of photo-isomerization.

Photo-isomerization presents a light-induced chemical process during which a substance passes into another, so called isomeric state. In this state the substance has the same chemical composition as in the initial state but differs in polarizability of its new form molecule. Macroscopically this results in light-induced change of the refraction index of the medium. The reactions of isomerization may be of a thermal and quantum nature depending on the way the reaction is run. Correspondingly, the character of the isomerization reaction determines the characteristics of the hologram-recording process in the substance. Most interesting for dynamic holography are the materials showing reversible isomerization reactions. This means that the material returns in its initial state via relaxation (the back isomerization reaction) or by means of an additional external impact.

The great variety of known polymer materials has now resulted in enormous quantity of publications devoted to holographic applications of these materials. In the present survey we, however, confine ourselves to consideration

of the media showing sufficiently high speed of the recording/read-out cycle since the response characteristics are of great importance for solution of our task.

2.5. Photorefractive polymers

Many of polymer materials exhibit photorefractive features. As is known the phenomenon of photorefraction is based on the combined effect of photo-conductivity and nonlinear optical properties of the material. Under exposure to light the non-equilibrium charge carriers are generated which then drift from an irradiated area to dark ones until being captured by traps. As a result the electrical charge field is set in the material. This field produces change of the material refraction index via electro-optical effect.

The photorefraction process in polymers differs from that in inorganic crystals in that the generation efficiency and mobility of the charge carriers in polymers are strongly dependent on the external electric field applied. Table 2.1 exhibits for comparison the photorefractive features of inorganic and organic materials.

Table 2.1. *Properties of inorganic and organic photorefractive materials.*

Property	Inorganics	Organics
Charge carrier photogeneration	Field independent (except for the high field Poole-Frenkel limit)	Strongly field dependent (Onsager model)
Charge carrier transport	Mainly diffusion (ferroelectrics) or conduction band drift with field independent mobility (simiconductors and selenites)	Weak diffusion. Electric field drift with field dependent mobility transport through localized (hopping) or quasiextended (narrow-band) states
Electrooptic activity	Ionic (ferroelectrics) and electronic (semiconductors) origins	Electronic origin
Dielectric constant,ε	Usually large r_{eff} is accompanied by high values of ε	Due to localized nature of electronic properties ε is usualy small
Sensitivity figure of merit, $n^3 r_{eff}/\varepsilon$	Limited to the range 1-20	Can be ~10^2 and more

The polymer materials optimized for the photo-effect meet requirements substantially differing from those the accustomed nonlinear materials do. Let us consider these differences in detail.

- To control both light absorption and its wavelength range, the proper photosensitive dopants in required concentrations are introduced into the

polymer. This results in better characteristics as compared to those of the original material.

- Though the polymer structure can itself support the charge-carrier transport from the irradiated areas of the material to dark ones, the special transporting molecules are introduced into the polymer's matrix.
- To increase the spatially-distributed-charge field, though it is set without traps, the proper dopants with the required energy of ionization acting as trap centers are introduced in polymers.
- Finaly, to increase the second-order electro-optic effect which may be inherent in the polymer itself, the chromophores showing the second-order activity are introduced in the polymer matrix. This also proves to be more profitable for the choice of the working spectral range of the material.

It should be noted that all the stages of the photorefractive process can be optimized simultaneously and almost independently. With this, the optimization degree absolutely exceeds that for the existing inorganic crystals.

The diffraction efficiency of refraction-index holographic gratings recorded in a photorefractive polymer is strongly dependent on the applied electric field since all the stages of development of the photorefractive process depend on it.

Photorefractive polymers (PRP) are characterized by sufficiently high values of diffraction efficiency and, depending on the polymer composition, by great variety of response time values.

The PRP based on poly(N-vynilcarbazole) (PVK) containing as a nonlinear optical chromophore 4-(N,N-diethylamino)-(β)-nitrostyrene (DEANST) was studied in [5]. As a photosensitive component was used, depending on the wavelength of the recording light, either fullerene C_{60} or thiapyrylium,4-(4-dimethylaminophenyl)-2,6-diphenylthiapyryliumperchlorate (TPY). Holographic gratings were recorded by light with the wavelength of 645nm in the composite comprising fullerene and with the wavelength of 703nm in the composite comprising TPY. The diffraction efficiency of the grating recorded in these materials amounted to 1-2%, and the response time was in the millisecond range (of the order of 100 ms).

The experimental results of the photorefractive feature study of a number of PRP are presented in [6]. The thickness of all the samples was of 105μm. The polymer was placed between two transparent electrodes. The recorded gratings presented volume holograms. The recording-light wavelength was changed from 633nm to 830nm. The power density of the recording beams varied in the range of $0.28W/cm^2 \div 0.7W/cm^2$, reading-out beams in the range of $0.6W/cm^2 \div 1W/cm^2$, and the external electric field strength in the range of $30V/\mu m \div 65V/\mu m$.

The maximum diffraction efficiency reached 10% ÷ 86% in different samples. The dynamic features of the samples were studied as well. They were characterized by both the temporal interval of recording of a hologram, which

amounted to several seconds, and the response time (the diffraction efficiency changing from zero to 1%), equal to about 0.8s.

The results of the study of the temporal characteristics of the photorefractive polymer composites containing poly-N-vynilcarbasole (PVK), N-ethylcarbasole and (2,4,7-trinitrofluorenylidene)malonodinitrile (TNFDM) with the chromophore of fluorinated cyano-tolan type are presented in [7].

The employed there chromophore is, in contrast to many other ones, transparent in a broad spectral range from far UV to near IR. It possesses maximum absorption at wavelength λ=342nm and low absorption up to λ=1μm. The studied composites proved to be fastest among the known PRP with very various in nature chromophores. At mean levels of both the intensity of light beams and electric field strength, the photorefractive response time amounted to 7.5ms, and at high levels of the mentioned fields to 4ms [7]. The orientation response time for this chromophore amounted to 490μs. At the electric field strength of 95V/μm the diffraction efficiency of holofraphic gratings was obtained equal to 24%.

It should be also noted the devices based on liquid crystals deposited on photo-conductive polymers [8-10]. The authors showed that azo-dye molecules introduced in a nonlinear liquid crystal (NLC) under exposure to Ar-laser radiation with λ=514nm were involved in the trans-cis photo-isomerization reaction [11]. This reaction resulted in reorientation of the NLC molecules was that allowed recording of dynamic polarization holograms. Khoo with co-authors observed a director axis orientation effect induced by the space-charge field in NLCs doped with dye molecules [12-14]. This mechanism of holographic grating formation is similar those occurring in photorefractive crystals. The corresponding effects are referred to as "orientation photorefractive effects".

In [15] was studied the process of holographic grating formation resulting from interaction between the spatial charge field and photo-conductive polymer layer under irradiation of two interfering light beams. The authors made sure that the main role in recording of the hologram played the electro-optical effect related to reorientation of NLC molecules under the action of the spatial charge field. The time of the grating growing up to the maximum magnitude amounted to 0.5s, and the relaxation time was of about 0.2s. Since the time of molecular reorientation amounts, according to the authors' estimates, to ~ ms at the presence of electrical field, the main contribution in the recording/relaxation dynamics in this material is of the processes of photo-generation and transport of charge carriers, and absorption of them by traps. The spatial period of the grating amounted to ~ 10-15μm. With this, the diffraction efficiency was obtained of about 10% at the applied electric field voltage of ~400V.

2.6. Azo-dye doped photopolymers

Last decades the photosensitive polymer composites consisting of azo-dye doped polymers become very popular [16]. These materials designed as thin films can be used repeatedly to execute thousands record-read-out-erase cycles in real time without any additional chemical treatment.

The basic recording mechanism in this materials is the well known light-induced reaction of trans -cis isomerization (see [17]).

At room temperature the trans -isomer is stable. However under exposure to light the molecular form changes resulting in the cis-isomer. The substance can return to its initial state (trans-isomer) after exposure either to darkness or to the light with a wavelength beyond the absorption band of the trans-isomer.

Fig.2.1 shows schematically the trans-cis photo-isomerization mechanism of azo-dyes.

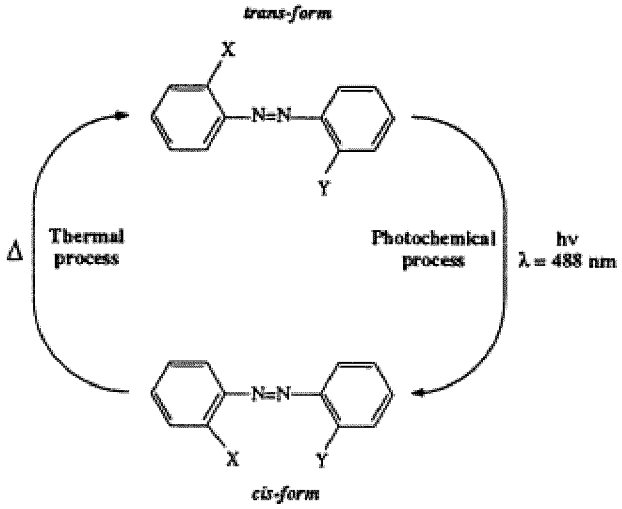

Fig.2.1. Trans ↔ cis photoisomerisation mechanism of azo-dyes. (X and Y being arbitrary molecules).

In [16] were studied polymethylacrilat polymer composites doped with five novel dyes AZD1÷AZD5. A schematic diagram illustrating the process of fabrication of PMMA matrix with an azo-dye is shown in Fig.2.2. Since these dyes have their absorption maximum in the range of 400÷550nm, for recording a hologram in [17] the light of Ar laser with the wavelength of 488nm was employed. Owing to that the azo-dyes show no absorption for the light with wavelengths longer than 600nm the read-out of the hologram could be executed with a He-Ne laser beam (632.8nm). The spatial frequency of the recorded holograms amounted to $1000mm^{-1}$. Most attention there was given to diffraction efficiency of holograms recorded in real time.

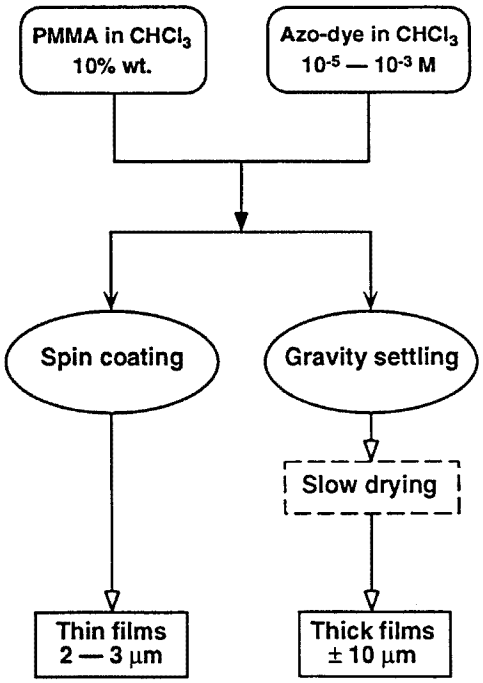

Fig.2.2. Schematic diagram of fabrication process of the azo-dye doped PMMA matrices.

The characteristic times τ_{rise} and τ_{decay}, and the diffraction efficiencies η obtained for the samples studied are presented in Table 2.2.

Table 2.2. *Characteristics of the azo-dye doped PMMA samples.* *(λ_{write} = 488 nm, $E_{total} \cong 32.5$ mJ/cm^2, λ_{read} = 632.8 nm).*

Azo dye	[AZDx](M)	τ_{rise} (s)	τ_{decay} (s)	η_{max} (%)	Max#of WRE cycles/50 s
AZD1	$1.0x10^{-3}$	3.3	7.6	3.7	33
AZD2	$1.0x10^{-3}$	3.2	4.1	5.1	44
AZD3	$1.0x10^{-3}$	3.5	14.2	10.1	44
AZD4	$1.0x10^{-3}$	7.4	5.8	0.1	13
AZD5	$0.2x10^{-3}$	3.4	13.3	1.5	33

Here WRE stands for "write-readout-erase", and [AZDx](M) for the azo-dye concentation.

The recording time was accounted as the time interval of the diffraction efficiency change between the levels of 10% and 90%.

The minimal exposition time for observation of the first-order-diffraction beam was of 100ms. Fig.2.3 shows the series of the hologram-recording cycles at exposition of 3s.

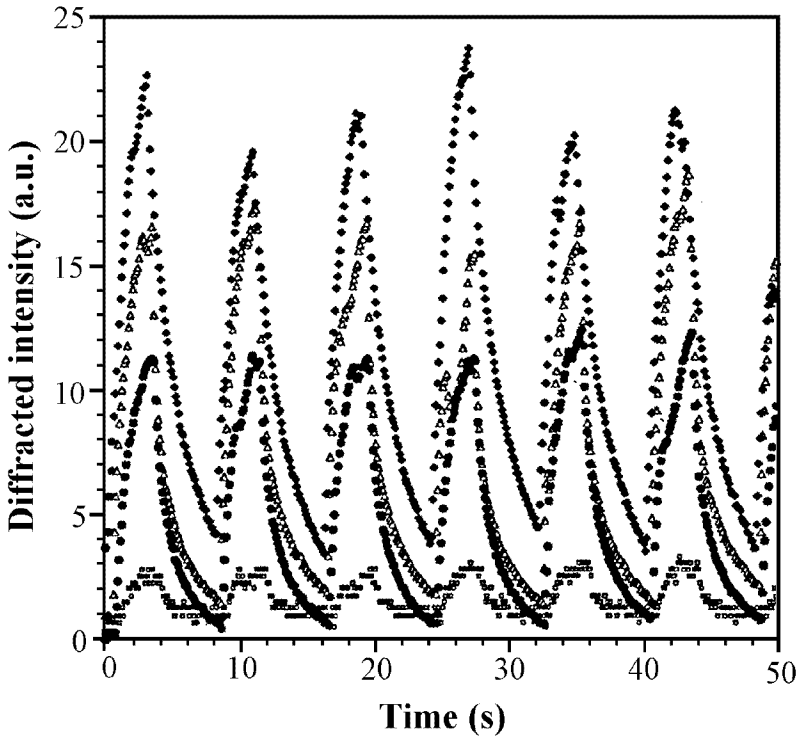

Fig.2.3. Numerous sucessive WRE cycles recorded on the different samples [17] (Exposure time = 1s with an interval of 3s).

2.7. Polymers with photochrom dopants

The polymers with photochrom dopants present a class of sufficiently prospective materials for holography. These materials possess the recording mechanism based on photon processes, and owing to it, they have advantages such as fast recording, high spatial resolution and density of information registered [18]. A significant class of photochromic materials described in [19] is that of spiropyrans. Their molecules comprise two π-electron moieties orthogonal to each other and in their conventional state are colorless. When the molecule is exited by UV light the C-O molecular bonds undergo cleavages, the π-moeities design the structure close to a plane one, referred to as the merocyanine form. Photochemical features of spiropyrans associate with this reaction of opening their molecular rings. This reaction results in a large spectral shift between the exited state of the substance (merocyanine form) and its basic state.

The characteristic feature of these materials is that the information registered in them may be erased due to thermal reactions after a short period of time even at room temperatures. Photo-induced reversible color changes between the thermally stable and metastable molecules of the spiropyran may lead to both spatial modulation of absorption and refraction of the polymer film. Owing to this, spiropyrans can be used for reversible recording of dynamic holograms. Note that recording can be executed in both the basic and exited metastable states of the substrate. A disadvantage of spiropyrans is that each of the mentioned states may undergo another reaction of isomerization which lead to an irreversible state. In

[19] the polymer films MMA and PVC doped with spiropyran 1,3,3-trimethyl-spiro-8-nitro(2-H-1-benzopyran-2-2-indoline)) were studied in application to the reversible holography. Exitation of the metastable state of the material was produced by UV light, and relaxation to the basic stable state by red light. The recorded gratings were read-out by Ar laser light with λ=488nm. The maximum diffraction efficiency for the film PVC 12μm in thickness was obtained of 10.5% and for 50μm of 0.43% at exposure energy of 300mJ/cm^2. The spatial frequency of holograms was 1718mm^{-1}. Unfortunately, the authors presented no data concerning the rise time of the grating for the 12μm thick sample. For the film of 50μm thickness this time, as seen in Fig.2.4 [19], amounted to units of seconds.

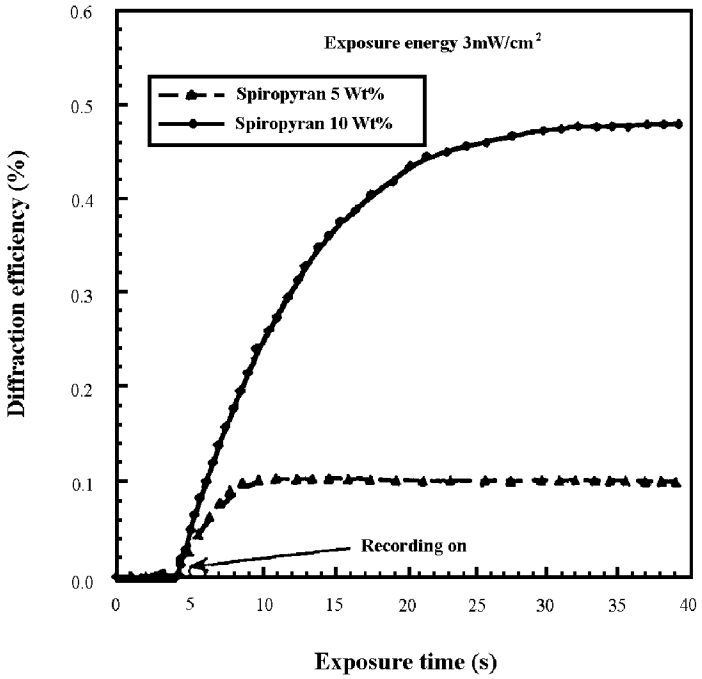

Fig.2.4. Influence of the concentration of SP on the real-time diffraction efficiency. Film thickness = 50 μm.

2.8. Nonlinear optical polymers

One of prospective classes of polymer media for dynamic holography is that of nonlinear optical polymers. Of most interest are those which molecules possess large effective length of π-π^*- conjugation that enable fast excitation of electrons and their effective movement along macro-chains. It was shown [20,21] that the cubic nonlinearity of a polymer is the more the longer its length of π-π^*-conjugation.

Just this case is when the donors (metoxiamino groups) are connected to one end of the molecule and the acceptors to another one (nitro- and cyano-groups). At the same time it is known that with increasing of the π-π^*- conjugation chain length the light absorption of the material is also growing that leads to

overheat and destruction of the polymer. In addition, the conjugated polymers are usually insoluble that restricts their functional potentials.

In [22,23] the nonlinear chromophores were attached to polymer chains forming thus the nonlinear polymers. There were used chromophores with a complex conjugated structure consisting of comparatively short molecules. Those chromophores were capable of photochemical transformations and formation of quasi-conjugated states under laser irradiation. In those papers the polymer chains were formed by the epoxy-monomer based on diglycidyl-ester of bisphenol A (containing of about 20% of epoxy groups). As a nonlinear optical chromophore was used 4-aminoazobenzen, being capable of photochemical transformations, in particular, trans-cis isomerization reaction. It formed the nonlinear optically active side groups joined to each monomer molecule by covalent bonds. Basing on experimental data, the authors concluded that opening of molecular rings of the epoxy-monomer occurs in the polymerization process resulting in new functional groups OH and C=O in macromolecules as well as new hydrogen bonds. Increase of the number of active OH groups advantages polymerization of the substrate in three dimensions. This forms a 3D-chain structure as the base for new quasi-conjugated states.

The holographic gratings were recorded in the material considered with the second harmonic pulses of YAG:Nd laser radiation. The pulse duration was 20ns. At least two nonlinear recording mechanisms of refraction-index gratings were found out experimentally which appreciably differed in relaxation speed. The time of the "fast" relaxation could reach 20ns, the maximum value of nonlinear susceptibility being $\chi^{(3)}=5*10^{-8}$esu. The "fast" relaxation was followed by the "slow" relaxation with the erase time about tens microseconds. Those effects resulted from electron (fast) and thermal or photochemical (slow) nature of the refraction index variation. The diffraction efficiency of the grating recorded by the beams of total energy of 0.4mJ in the sample 140μm in thickness was obtained of 20%. With this 8 diffraction orders were also observed. Fig.2.5 presents the temporal characteristics of the recorded grating relaxation. As is seen in Fig.2.5, the relaxation time corresponds to the microsecond range.

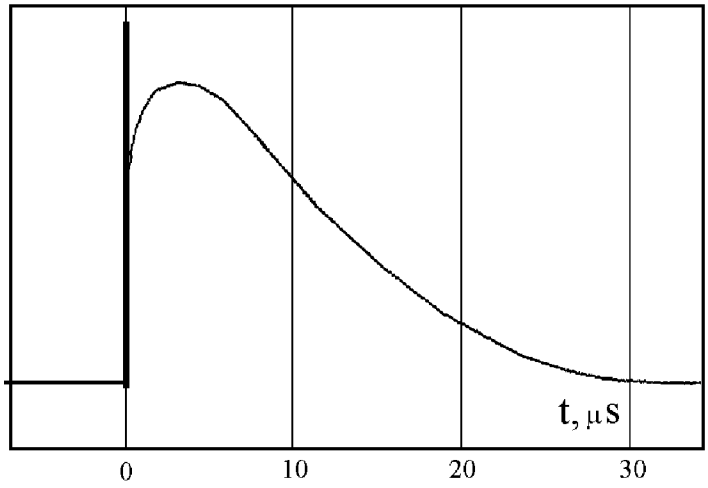

Fig.2.5. Oscilloscope trace of the dynamic grating relaxation.

In addition the reversible gratings with the relaxation time of about 10-15 hours recorded with light pulses of nanosecond duration were also observed in the experiments. The recording mechanism started acting at intensity of light beams of 300kW/cm^2 and higher. With this the maximum diffraction efficiency reached 15%, up to ten diffraction orders being observed. No changes in transmittance of the medium were noticed. The grating was recorded with a single laser pulse of intensity I=0.8MW/cm^2 at λ=0.53μm. Then it was read out with CW He-Ne laser radiation. Erase of the grating was executed with one of the recording beams of intensity I=2MW/cm^2. In the authors' opinion, this mode of recording/relaxation of holograms owes its existence to the trans-cis isomerization [24] of the aromatic components. This is caused by light-induced rotation of one part of a chromophore molecule around of the double bond N-N [24-26]. The trans-cis isomerization time depends on the medium that serves as a chromophore solvent and can amount to minutes or even hours. Kinetics of the process is very complex and has not yet studied sufficiently.

Thus, the considered polymer structure is suitable for both design of optical memory devices and dynamic holography applications.

Concluding this survey of polymer holographic materials, we would like to note that one of appreciable problems arising when one chooses a proper material for recording of the membrane mirror hologram is that of mechanic and thermal-mechanic features of the materials. The issue of great importance is also how the mentioned properties of the material affect the optical characteristics of the hologram recorded.

Unfortunately, the information of this sort is extremely rare in the publications devoted to holographic studies. So we consider the paper [27] being noteworthy in which the effects of mechanic features of Dupont polymers on their optical properties were studied. The authors studied characteristics of both a

device as a whole and its components, namely, of the polymer layer and the mylar film served as the substrate and the coating for the polymer. Experimental study involved measurements of thermal extension and residual tensions of the material, adhesion of the film components to each other, and influence of device deformations on the diffraction efficiency of recorded holograms. As a result it was found that the device as a whole showed dynamic mechanical characteristics close to the corresponding characteristics of the mylar film.

2.9. Biological photomaterials

There is a class of media of biological origin which deserves to be particularly marked among organic media for holographic applications. These media are characterised by their polymorphism which extends their range of potentials for recording of holograms. Photochromic properties of these media enable one to record reversible diffraction structures.

A characteristic sample of this class of media is a substance investigated well enough – bacteriorodopsin (BR). The BR is a trans-membrane protein which is synthesised by bacteria Halobacterium salinarium [28,35]. The nonlinearity formation mechanism in BR is conditioned by spatial charge re-distribution. This results from displacement of a proton exposed to light from the citoplasmatic side of the membrane to its periplasmatic side [28,29]. The BR belongs to reversible holographic media, and what's more, resumption of the initial optical characteristics of the medium might be of either spontaneous or stimulated nature. For holographic applications two states in the BR photocycle are of most importance [29,30,33]. These are referred to as B-state and M-state. Being in the basic state B (otherwise trans-state), molecules of BR absorb light effectively in the spectral range of 400nm÷700nm, having the absorption maximum at the wavelength of 570nm [30-32]. The absorbed light energy produces excitation of BR to the metastable M-state (otherwise cis-state). Used most frequently for recording holograms, this state is characterized by the absorption spectral range of 300nm÷500nm with the maximum of absorption at the wavelength of 412nm [31,32]. The molecules return from the cis-state to the trans-state via spontaneous or stimulated relaxation (depending on conditions of the holographic 'record–read-out–erase' cycle).

The trans-cis excitation (B→M transition) and cis-trans relaxation (M→B transition) processes in BR are separated in spectrum. That is why the medium allows forming of two types of gratings: B-type arising from the spatially modulated B→M transition, and M-type corresponded to the M→B transition spatial modulation. The lifetime of gratings recorded depends on numerous factors and varies within a wide interval. In [32] the B→M transition time (B-type grating) measured 20sec, and the M→B transition time (M-type grating) – 0.5ms. In the latter reference a polymer film contained BR was used as an experimental sample. In the same reference an attention was paid to the M→B transition-time

dependence of the exposure intensity at the wavelength λ=412nm. In [31] the M→B spontaneous relaxation time was given which amounted to ~10ms for the standard biological quality sample. In the same reference the fact was marked that either introduction of BR being in a suspense state into a polymer matrix or adding some chemical agents to the solution might prolong M→B transition time to 1-2hrs.

What is valuable for the reversible holography, the gratings recorded in BR can be fast erased being exposed to blue light which causes the direct transition of the substance from the M- state to the B-state. This allows one to accomplish a cyclical process of recording-readout-erasing in sufficiently short timeframes. Fig.2.6 [35] presents such a cycle having 1.2sec period and the recording/erasing times of ~130ms. High spatial resolution, which exceeds 5000mm^{-1}, and fairly good sensitivity ~10^{-3}J/cm^2 [33] should be related to the advantages of this medium. Refractive index variations depend on many factors, e.g. exposure intensity, and can reach ~10^{-4} [34].

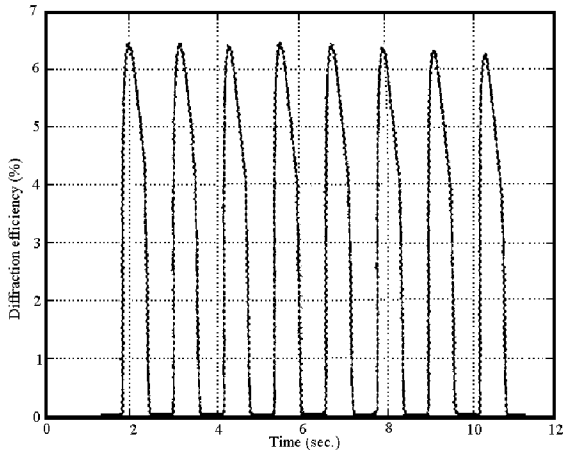

Fig.2.6. A pulse train by three-laser-beam transient holographic technique [35].

The diffraction efficiency of holographic structures recorded can amount to units of percents in some experiments [31,35], which is a characteristic feature of BR among the media of biological origin. Thus in [35] the maximum diffraction efficiency of the hologram was of ~7% at the recording light intensity of 31mW/cm^2 and the exitation light intensity of 13mW/cm^2. The experiments carried out [35] showed that the stationary diffraction efficiency of gratings in BR as well as their relaxation times depend on the both recording and exitation beam intensity and can be optimized by means of the correct choice of the ratio of the beam magnitudes.

Extremely high stability to chemical, thermal and photochemical influences also relates to advantages of this material. It is noted in publications that the holographic 'record – read-out' cycles more than 10^6 in amount, resulted in no deterioration of the substance characteristics. [31,35]. It is also important that BR

can be easily modified genetically as well as chemically to give it the properties required for the concrete applications.

2.10. On applicability of reversible photothermoplastic process for recording of dynamic holograms on membrane mirrors

At present the photothermoplastic (PTP) process has been developed in detail and is used in imaging telescopic systems for image registration of the observed objects. Naturally, the optimum version of the system is that which modulation transfer functions of both the optical system and the image detector are very close or the same. From this standpoint, classic haloid-argentum photomaterials with improved resolution approach to optical systems in their resolution. However, these materials have one essential demerit. It is extremely difficult to transfer efficiently information from them in real or close to this time scaling.

It should be noted that electronic detectors aimed at image registration, which on the contrary can actively transfer the information, possess rather low resolution compared to photomaterials.

In several recent years the detectors for image registration were developed at Vavilov State Optical Institute [36,41]. They combine the best features of both photomaterials and electronic detectors, such as high resolution with sufficient sensitivity, typical for photomaterials, and operational efficiency of image transfer inherent in electronic detectors (e.g. [36]). These detectors are based on the PTP process and thus on PTP materials.

A consistent PTP process in double-layer materials with an injection photoconductive layer (based on Se and Te alloy) and also with a transporting thermoplastic layer made of an organic polymer composition appeared to be the most prospective.

The developed PTP-process theories and the technologies of PTP materials have allowed designing of reversible photosensitive films up to 190mm in width with the following characteristics:

- The sensitivity spectral range spreads from 400nm to 750nm (with decrease of sensitivity not more than three times of the maximum value), the spectral characteristic having its maximum within the range of 450nm÷550nm and monotonous drop in the longer wavelength direction.
- Holographic sensitivity (for diffraction efficiency being of 1%) corresponding to the spectral characteristic maximum attains $2\times10^7 cm^2/J$.
- The limiting spatial frequency of the grating recorded is not less than $1200mm^{-1}$.
- The minimal time of the 'record-erase' cycle does not exceed portions of a sec.
- Durability of the record-erase process attains 300÷500 cycles.

- The dynamic range provides the performance at exposure changes of more than two orders of magnitude.

However, PTP materials are not free of several drawbacks. They are

- a high-voltage corona discharge in gas needed at the stage of sensitization;
- dependence of optimum time of latent image development on spatial frequency of the image (that results in difficulties on registration of the images containing low spatial frequencies along with high spatial frequencies);
- a limited record - erase cycle number;
- technology complexity of fabrication of large-area multi-layer thin films, uniform in thickness.

Having in mind reversibility, high sensitivity and resolution of PTP materials and their possible DOE application in the membrane primaries of imaging systems, we consider it noteworthy to mention a number of additional requirements to these materials, arising from the peculiarity of the task. They are:

- minimum duration of the 'record – read-out – erase' cycle (by reduction of the recording and erasing stage duration),
- increase of the permissible number of 'record – erase' cycles without any deterioration of DOE's optical characteristics,
- development of methods of uniform heating the large-area thermoplastic-layer surface adjacent to the substrate,
- development of the technology of application of PTP material layers, uniform in thickness, to large-dimension mirrors.

The peculiarities of the PTP process make difficult or confined its application in conditions of the vacuum and low or non-uniform heating. Thus, transition of a thermoplastic to its liquid phase in the vacuum may cause its enforced evaporation from the substrate. The electrostatic sensitization needs in corona discharge in gas. The comparatively low melting temperature (100^{o}C) of thermoplastics requires rather accurate and uniform heating regime over the whole surface of the primary mirror.

The physical processes taking place at various stages of PTP registration were studied theoretically and experimentally by a number of researchers (see e.g. [37-39]). The PTP process can be conditionally divided in several stages, for the sake of convenience referred to as follows: charge sensitization, exposure, developing, fixing, reading out the information recorded, image erasing. This cycle is repeated completely with the required periodicity.

The typical PTP material presents a thin double- or triple-layer structure, placed onto a dielectric substrate which can also be in a particular case a flexible membrane having a reflective coating on its backside. Such a membrane can be used to design an elastic membrane primary mirror. On the membrane's side free of the reflective coating, a thin transparent conductive heating layer is applied on which the injection and transporting thermoplastic layers of PTP material are placed consequently.

A PTP material operates in the following way:

- During the sensitization stage with the help of a high-voltage corona discharge from the special electrode placed at the face side, the formation of the surface uniform electrostatic charge occurs on the external layer of the thermoplastic.
- Under exposition to light in the working spectral range, defined by the properties of the photoconductive injection layer, the charge stored earlier partially runs down in the exposed places of PTP film. With this the potential relief on the film surface is formed, modulating the inner field intensity in the thermoplastic and thus shaping the latent image of the interference pattern.
- The developing stage is photothermoplastic temperature increasing (up to hundreds degrees centigrade) with the use of either the heater (passing a pulse current through the conductive heating layer placed directly on the substrate) or a separate heat source (in a contact or radiating way). At the developing stage the latent image is converted into the real one as the surface relief resulting from the impact of non-uniform surface electrostatic forces on the thermoplastic heated up to its semi-liquid state. The electrostatic forces compress the thermoplastic layer whereas the surface tension forces trend to smooth the relief arising on the surface. At the beginning of the developing process, the electrostatic deformation forces prevail. When the developing time exceeds the optimum interval, the relief becomes smooth and the diffraction efficiency of the phase structure obtained starts droping due to the surface tension forces acting in the liquid thermoplastic.
- The reading-out stage is decoding of the relief-phase structure registered with the help of a probe light beam. This stage is executed after the thermoplastic layer has cooled down to its initial temperature due to the material thermal conductivity on switching off the heater at the moment of optimum developing. The time of keeping of the information registered is practically unlimited since the surface relief is remembered owing to transition of the thermoplastic layer to its solid phase.
- The cycle ends by the erasing stage. This stage embraces the repeated heating of the thermoplastic up to a higher temperature at which the surface tension forces smooth the surface relief and restore a flat-layer surface. Then after cooling the PTP material becomes ready for a new record – read-out cycle.

At present the PTP layers based on principally new media, namely, compositions of nanocrystals of inorganic and organic semiconductors inside of

polymer structures have been developed at the Vavilov State Optical Institute [40]. Earlier the photosensitive media used comprised micro-crystals of either inorganic (Cadmium and Zinc sulphides, Cadmium selenide, Zinc oxide et al.) or organic (dye) semiconductors in the polymer binders. The layers of this sort are easily applied to substrates and exhibit high sensitivity to light, but being strongly scaterring media (microcrystal's size is about 1μm), show low resolution. On the contrary, certain amorphous media exist having rather good resolution but usually low sensitivity to light.

It was to combine the positive features of these materials the technology of nano-crystal media had been developed for.

The attractive potentials related to the new PTP materials are feasibility of the easier technology of single material layers, possibility of improvement of reproducibility and uniformity of the film characteristics over the whole surface, possibility of application of PTP materials to both rigid and flexible large-area substrates.

The results considered of theoretical and experimental investigations of PTP materials allow us to evaluate their potentials in the application for recording dynamic DOE.

We believe that in spite of all the difficulties mentioned above the PTP technology might be feasible in development of dynamic holograms on the membrane primary mirrors of imaging systems with holographic aberration correction.

2.11. Nonlinear properties of fullerene doped photosensitive materials

In this section we will briefly consider the properties of polymer materials doped with fullerenes in connection with special attention paid to these materials during the last decade.

Since the discovery of fullerenes in 1985 [42] there were a lot of publications on their investigations including those on their nonlinear optical properties. At present there exist the detailed reviews on this topic [43-46]. Feasibility of recording holograms is one of the attractive directions of fullerene applications in nonlinear optics.

The fullerenes may exist as liquid and solid solutions, can be introduced as dopants in porous glasses, polymers, liquid crystals, and also can form thin films. At present the properties of the fullerenes of C_{60} and C_{70} type have been studied most completely. Nonlinear properties of the fullerenes are specified by the structure of their molecules. The spectral region, where the nonlinear properties of fullerenes are displayed, lies within the wavelength range 400nm÷700nm for C_{60} and for the higher fullerenes C_{70}, C_{78}, C_{84} is shifted to the wavelengths longer than 700nm [47].

The fullerenes can be applied to recording of amplitude and phase dynamic holograms with the use of mostly pulsed laser radiation, though sometimes it might be CW radiation as well.

Under exposure to irradiation the absorption ability of polymers doped with fullerenes raises with increasing of the exposing light intensity. This phenomenon is named an reverse saturable absorption (RSA). It can be used for recording of amplitude dynamic holograms. The RSA phenomenon is of threshold nature. The threshold values of the energy density W under pulsed exposure increase with pulse duration increasing and these are of 10^{-3}J/cm^2 in rate within the nanosecond duration range [48,50]. The least threshold intensities allowing RSA in these media were observed in [51] with the use of laser radiation of λ=532nm and pulse duration of about 15ns-20ns. The nonlinearity threshold for C_{70} in NChLC was less than 250μJ/cm^2 (I<10^4W/cm^2).

Theoretical and experimental investigations showed that the RSA process is accompanied by photoinduced processes of defocusing and light scattering [52,53] associated with the refraction index variations in the medium. The refractive index variation results from two factors: molecular polarizability and medium heating. In the opinion of the authors of [45], the refractive index variation specified by heating is an order of magnitude greater than those conditioned by the molecular polarizability. The variation of the refractive index Δn being proportional to the exposing light intensity, was observed in [49] where RSA was studied in a thin film (0.6μm in thickness) of C_{60} exposed to He-Ne or Ar-laser CW radiation having intensity of ~10^3W/cm^2. In this case the proportionality factor was equal to 1.4×10^{-3} cm^2/W and $\Delta n=-3\times 10^{-5}$.

Direct holographic experiments on recording and reading out of dynamic holograms were carried out in [47] in polymer films of polymetylmetacrilate (PMMA), containing C_{60}. The hologram was recorded by single frequency radiation of second harmonic of Nd laser (λ=532nm). The energy and pulse duration were 5mJ and 10ns correspondingly, beam diameter being 11.5mm. The angle between the intersecting beams in the hologram plane was of 16mrad that corresponded to the hologram period of 33μm (30 lines per mm).

The radiation intensity may be varied within 1MW/cm^2-100MW/cm^2 and the energy density within 10mJ/cm^2-100mJ/cm^2. In the experiments self-diffraction of the laser radiation was observed. The process of recording the hologram was of threshold in nature and what's more, the hologram formation threshold was by the order of magnitude lower than the RSA threshold. Some of first self-diffraction orders were observed at I=2.5MW/cm^2-5MW/cm^2 (W=25mJ/cm^2-20mJ/cm^2). At I=20MW/cm^2-30MW/cm^2 there were 5 orders observed.

A few words should be said about fullerenes nonlinear properties while these were introduced into conductive polymers which possess intermolecular charge trasfer under the light exposure [54,55]. It was noted [55] that transferring

charge polymers, doped with fullerenes, are of a new class of materials for nonlinear optics applications. These allow one to produce extremely fast recording of holograms including that with the help of single pulses of a femtosecond duration. A charge conveyance from the conductive polymer to C_{60} molecules is executed in times of the order of 300fs [55]. In the noted reference the phase hologram recorded on refractive index variations in the sample was read out and the signal transmitted through the sample was observed in the experiments on RSA. The sample presented a thin film of good optical quality of poly [2-metoxy, 5- (2'ethylhexoxy)- 1,4-phenylene vinylene] (MEH-PPV) doped with C_{60} of various concentrations. A Ti:Sapphire laser radiation (λ=800nm) with the pulse duration of 150fs was applied for excitation (in the RSA experiment) and for reading out the hologram, and its second harmonic (λ=400nm) was used for recording the hologram. Such a choice was specified by the fact that the recording wavelength was close to the absorption peak of the sample, whereas the induced absorption in the sample had its maximum in the near IR region. Energy density W and radiation intensity I in the film plane (1mm^2 in area) was 3×10^{-4}J/cm^2 and 2×10^9W/cm^2 respectively. The diffraction efficiency $\eta \approx 1.6\%$ was achieved in the experiment. Investigations of time dependence of the variations of the sample transmission ΔT and the phase-hologram diffraction efficiency η showed that the manifestation of nonlinear phenomena in the medium is virtually instantaneous. In [54] the study results of nonlinear properties of thin films of poly(3- oktyl thiophene) - methanofullerene (6-7 μm in thickness on the KBr substrate with an admixture of C_{60}) are presented. The nonlinear effects were observed in the IR spectral range at the intensity of exciting CW radiation of 50mW/cm^2 (the 514nm line of Ar laser radiation). Those effects displayed very rapidly, whereas the relaxation was essentially slower (of several ms in rate). The changes of the imaginary and real parts of the refractive index value amounted to $\Delta K \approx 2.8\times10^{-2}$ and $\Delta n \approx +1.5\times10^{-2}$, respectively.

Completing the consideration of the fullerene doped polymers, we can conclude the following:

The main merit of these media is a high speed of manifestation of nonlinear phenomena under exposure to light. Developing and relaxation times depend on a type of mechanism (electronic, Kerr, electrostrictional or thermal) which specifies nonlinearity arising. These times can be from femto - to milliseconds [56]. Employment of single pulses of pico - and – femto- second duration for excitation allows reducing of the contribution of slow mechanisms (thermal, electrostrictional).

A drawback of these media is a high threshold of nonlinearity arising. Thus, in the nanosecond range the threshold intensity of exciting radiation was not less than 10^5W/cm^2 [50]. It should be noted that for fullerenes in NChLC used in [50] the threshold intensities appeared to be approximately by the order of magnitude lower. The uniquely low threshold intensities (~50W/cm^2) were achieved with

CW excitation (λ=514nm) in thin films of a conductive polymer containing C_{60} [54]. With this the maximum values of both the real part $\Delta n_{max} \approx +1{,}5 \cdot 10^{-2}$ and the imaginary part $\Delta K_{max} \approx 2{,}8 \cdot 10^{-2}$ of refractive index variation have been achieved.

Light scaterring, which is often observed in the experiments with fullerene doped media, can produce a negative influence on the optical quality of a beam passed through these media.

At present researches of media contained fullerenes are being actively developed, some interesting results have been already obtained and, apparently, the materials can be expected in the nearest future with their characteristics being superior to those of the existing materials.

2.12. Conclusions concerning prospects of application

The survey of the media appropriate for recording dynamic DOE and the carried-out analysis of their nonlinear mechanisms and characteristics important for the considered application have shown that a great number of nonlinear media allow recording DOE on membrane mirrors. There exist media possessing the required response speed, sensitivity, spectral range, diffraction efficiency of recorded holograms, potentials of application on large-area elastic films and adhesion capacity. However, no medium is yet available meeting all the requirements simultaneously. In this connection further efforts in search of nonlinear media and examination of their parameters are actual now to select the medium suitable for solving problems of dynamic holography similar to this related to the present Contract subject. In our opinion, nowadays the potentials exist sufficient for development of an organic nonlinear medium possessing the properties needed for solution of the problems of such sort.

Section 3. Fabrication of small-size samples of membranes with nonlinear optical coating

In the previous section of the present report a survey of nonlinear media suitable for recording of dynamic holograms applied to the membrane primary mirrors of telescopic systems is presented. The conditions of recording/read-out of the holograms, the achievable values of diffraction efficiency, spatial-temporal characteristics of a great number of nonlinear media have been considered, the most appropriate candidates having been chosen for the further experimental investigation. In this section we give a brief description of the samples fabricated to simulate the membranes with nonlinear optical coating.

Choosing the material for experimental demonstration of feasibility of recording/readout of a dynamic hologram in a nonlinear medium, applied on the elastic film surface, we were guided by availability of the material first of all (that is rather important in conditions of limited financing of the work). What's more, we were fully aware of that the medium chosen could not show excellent parameters in speed of response, sensitivity and diffraction efficiency. Taking this into account, we decided in favor of three materials as possible candidates, namely, a photothermoplastic, a fullerene doped polymer film, and a biological material based on the bacteriorodopsin.

3.1. Films with photothermoplastic layer

In purpose of testing the samples of films with PTP layer were fabricated. The transparent conductive tin-dioxide layer of about 2μm in thickness (of about 4Ohm resistance) and PTP layer based on a composition of semiconductor

nanocrystals in a polymer structure [40,41] (developed in Vavilov State Institute) were applied consequently on a mylar film of thickness of 150μm. The clear aperture of the samples was 40mm. The spectral sensitivity range of the media covered 0.4μm ÷0.75μm with the maximum in the region of 0.45μm ÷0.55μm. The sensitivity in the spectral characteristics' maximum reached 0.5×10^{-7}J/cm^2. The medium allows recording of holograms with the utmost spatial frequency of 1200mm^{-1}. Durability of the record/erase performance is to be not less than 300-500 cycles.

3.2. Fullerene doped PMMA films

Another candidate chosen for testing was a nonlinear medium that contained fullerene C_{60}. The merits of this medium according to the data published are a broad spectral range of nonlinearity, high speed of response, great dynamic range. As for demerits one could consider the threshold nature of the recording process and a relatively low sensitivity. These demerits are not of principal nature but offer additional requirements to the recording-light source.
For experimental examination some samples of polymer film of PMMA doped with fullerene C_{60} were fabricated. The films were about 200μm thick and had the clear aperture of 1×1 cm^2. The films were distinguished by concentration of the fullerene and consequently by their transmission of light. The transmission factor for the films exposed to the light of the wavelength of 0.532μm (Nd-laser second harmonic) amounted to 0.52, 0.74 and 0.81.

3.3. Films with BR

BR as a nonlinear medium for recording of dynamic holograms had been investigated in detail during last several years. This nonlinear medium proved to be stable for a long time, permits repeated the recording/erasing of the holograms, possesses high speed of response and sensitivity, high spatial resolution, can be applied to elastic substrates. However, comparatively low transmission in the visible spectrum, low diffraction efficiency of the holograms and appreciable light scattering confined the application area of this nonlinear medium. In spite of this we are going to carry out experiments with BR dissolved in glycerin.

Section 4 (5). Experimental demonstration on record/read-out of dynamic diffraction holograms on membranes with nonlinear-optical coating (*)

In this section we present the description of the main experimental results on studying the features of recording/reading out dynamic holograms on membranes having a nonlinear medium on their surface. We could not employ the media recommended in Section 2 of this report because of the limited terms and finance. Therefore we used in our experiments a thermoplastic and bacteriorodopsin.

4 (5).1. Thermoplastics

As was mentioned in Sections 2 and 3 of this report PTP-process has been quite well developed now both theoretically and experimentally. To carry out all the required steps of this process (sensitization, exposure, development and erase) we had in our disposal the specially designed electronic unit and the optical unit for exposing the PTP sample to coherent beams forming the diffraction structure required.

The block-diagram of the electronic unit and the optical unit are shown in Fig.4(5).1.

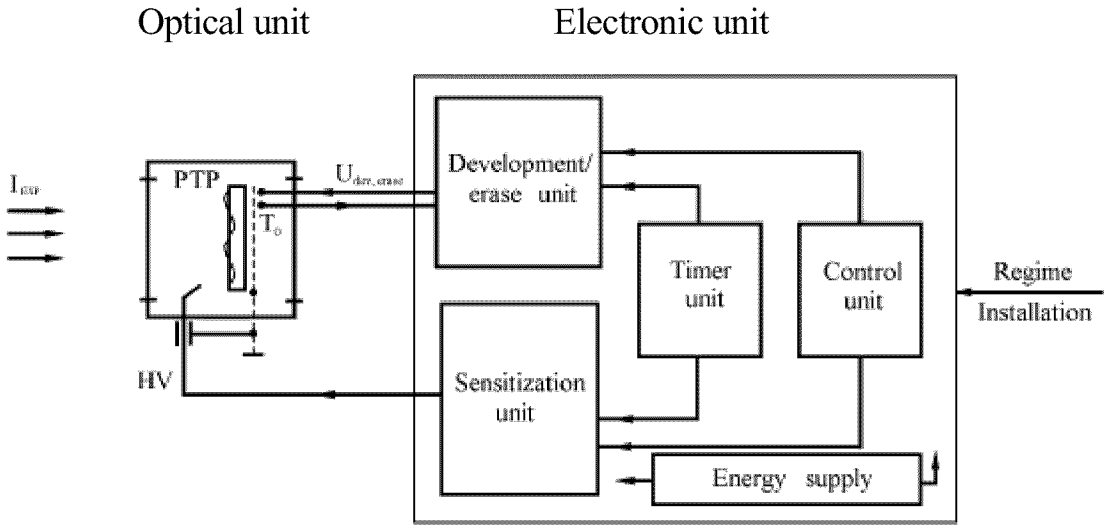

Fig.4(5).1. Block-scheme of apparatus for experiments on record/read-out of dynamic DOE in PTP material.

The experimental setup with the use of PTP is similar to that in item 4(5).2 excluding that here we used for recording DOE a CW Ar^+ laser beam of total

(*) Footnote: The dual numbering of the items in this section is related to that this section contains the results concerning the two corresponding items of the Contract.

power (in all spectral lines) of 2W. The laser radiation of power 0.8W at the wavelength 0.5145μm selected from its total spectrum (the selection way is well known and was described earlier) enters the PTP material in the optic unit through the electric-mechanic beam- shutter providing the needed exposure time. The recorded information was read out and measured as described in item 4(5).2.

The optimal regime for each step of the PTP process was chosen taking into account the concrete experimental conditions. We selected the needed voltage for sensitization of the material, the exposure light intensity, the PTP-layer temperature as well as its increase rate for developing the material, the erase temperature. Since the 'red limit' of the PTP-material spectral sensitivity lies in the range of 0.70-0.75 μm, we implemented the record/read-out steps separated in time.

We examined the sample of a single-layer PTP-material being a mylar film 150μm thick coated by a conducting tin-dioxide substrate (total resistance of 4.5 ohm). The injection layer of Se nanocrystals in the transport-thermoplastic layer of styrene and bivinyl copolymers composed with hydrazone and polyvinyl-carbazole was deposited on this substrate. The features of these PTP materials were studied in details and described in [40,41].

With the chosen optimal parameters of the PTP-process selected we have obtained the following typical results of reversible recording the diffraction structures:

- The diffraction efficiency (read-out at λ=0.63 μm) of 1.5%-2.0% at spatial resolution of 95 mm^{-1},
- exposure time of 1ms,
- the total recording time of about 0.3s,
- total abatement of the filters (see 4 in Fig.4(5).2) about $1.5 \cdot 10^5$ times (It corresponded to the PTP-material energy sensitivity $\approx 500 m^2/J$.)
- the erase time ~ 0.5s.

The experimental results obtained proved the PTP material to show rather high sensitivity and resolution capacity. Unfortunately, it has appeared to be fairly inert and thus suiting for compensation of only slowly varying (e.g. thermal) aberrations.

4(5).2. Bacteriorodopsin

The experimental schematic is shown in Fig.4(5).2. The beam of He-Ne laser 1 of power of 15mW is split by the beamsplitter BS1 into two beams to record the hologram. One of the beams (transmitted through the beamsplitter) reflects from flat mirrors M2, M4 and impacts the membrane (with the nonlinear medium applied) fixed in a special mounting 3. The other beam (reflected by the beamsplitter) reflects from flat mirror M3 and then directs to the membrane as the above does. The angle between the beams amounted to 6 angle degree, thus the interference pattern with 75 lines per mm was formed in the nonlinear medium.

For a higher contrast of this pattern the beam intensities were equalized with light filter 4.

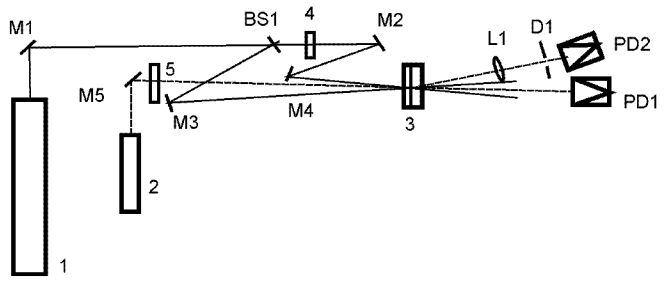

Fig. 4(5).2. The experimental schematic.

The hologram was read out with the beam of another He-Ne laser 2 (Fig.4(5).2) of power of 2mW. If required, the reading-beam power was reduced with light filter 5. The power of the beams in the zero and minus-first diffraction orders was registered by photo-receivers PD1 and PD2, respectively. To lower background irradiation, the Fourier filter comprising lens L1 with its focal length of 250mm and a 1m-aperture diaphragm in its focus was set in front of photo-receiver PD2.

This optical scheme was employed for experimental investigation of the process of recording/reading out dynamic holograms in bacteriorodopsin. This nonlinear medium was placed between two transparent 20μm-thick mylar films. The bacteriorodopsin layer thickness also amounted to 20μm. The films were fixed in the special mounting 3 (see Fig.4(5).2). The absorption coefficient of the nonlinear layer was 0.23 per a trip at the wavelength of 0.63μm. The recording-beam intensity was 3mW/cm^2, the hologram being read out with the beam of 0.2mW/cm^2. In these conditions the hologram diffraction efficiency amounted to 0.8%.

Fig.4(5).3 shows the measurement results of the temporal parameters of the hologram recorded in bacteriorodopsin. As is seen in the figure, the characteristic time of recording the hologram is virtually the same as the characteristic erase time equal to 0.18s.

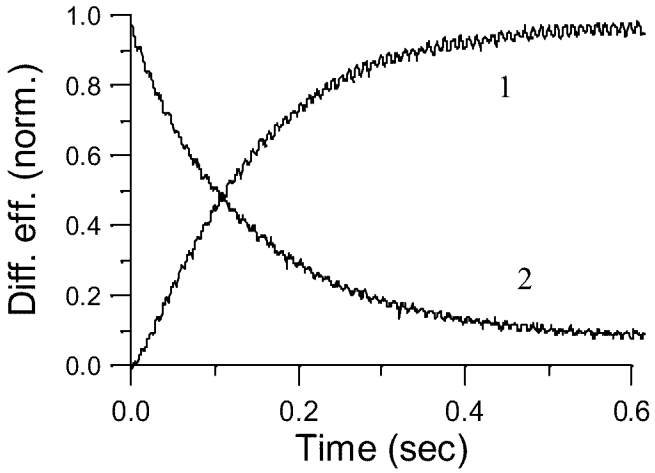

Fig. 4(5).3. Normalized diffraction efficiency of the dynamic hologram versus time during the recording stage (1) and the erase stage (2).

Thus, the presented results of the experimental study of conditions of recording/reading out the dynamic holograms on membrane mirrors show potentials of their usage in imaging systems with correction for PM distortions. Along with this the hologram parameters attained are not optimal ones. Obviously the additional studies are necessary aimed at searching novel nonlinear media for dynamic holography and also at improving sensitivity of the known media, diffraction efficiency of the recorded hologram, and speed of record/read out processes.

Section 6. Theoretical and experimental studies of stability of static DOE on the membrane mirror

In this section we present the main results of theoretical and experimental studies of function peculiarities of a static DOE applied on the membrane mirror surface, conducted in the framework of this Contract. The goal of the investigations was to find out the character and magnitude of the additional phase distortions conditioned by DOE deformations, to determine the allowable distortions of the membrane mirror with the DOE in dependence upon image-quality requirements and mirror parameters.

6.1. Theoretical analysis of deformations of static DOE on the membrane mirror

In [57] the task was solved of the surface deformation of a thin membrane with its circumference fixed at a uniform transverse load. In particular the longitudinal and cross shifts of the point with a coordinate r on the flat mirror under the pressure q along the membrane normal were given by the formulas [57]

$$U(r) = \frac{r}{a^2}\beta^2 \sum_{i=0}\left(\frac{r}{a}\right)^{2i} b_1^{1-3i} d_i , \tag{27}$$

$$w(r) = \beta \sum_{i=1} \left(1-(r/a)^{2i}\right) b_1^{2-3i} c_i^* , \tag{28}$$

where

$$\beta = \left(\frac{q\,a^4}{2Eh}\right)^{\frac{1}{3}},$$

a is the mirror radius, and h, E, are thickness, Young's module of the membrane material, respectively. The coefficients d_i, c_i* given in [57] depend only on ν (Poisson's ratio). The b_1 is determined by the boundary conditions. It is important to note that in the absence of a membrane-edge displacement ($U(a)=0$) b_1 depends only on ν. In the case of displacement or the force given at the edge b_1 appears to be a function of pressure, mirror dimensions, and material constants.

Using (27) and (28) one can consider the deformations of static DOE applied on the membrane mirror surface. Suppose that DOE is applied on the mirror with pressure q_o acting upon its surface. With this, the surface shape can be either spherical (convex or concave if $q_o \neq 0$) or plane ($q_o=0$). Let us also assume that the DOE is initially of ideal quality. Then a pressure variation on the mirror surface will lead to a surface shape change. Along with this, the DOE grating lines

will shift from their initial positions. The shifts of the lines will result in additional phase distortions due to the deformations of the DOE phase structure. Let us consider the appearance and magnitude of these distortions.

With pressure changing from q_o to $q_o+\Delta q$, the point with a coordinate r on the mirror (and hence the corresponding DOE line) acquires the shifts ΔU and Δw in the longitudinal and cross directions, respectively:

$$\Delta U(r, q_0, \Delta q) = U(r, q_0 + \Delta q) - U(r, q_0) , \tag{29}$$

$$\Delta w(r, q_0, \Delta q) = w(r, q_0 + \Delta q) - w(r, q_0) . \tag{30}$$

If the mirror's edge is fixed these amounts can be factorized into two factors. One, being a function of *r/a,* describes the radial-shift distribution. The other characterizes the shift magnitude and depends on the mirror's parameters and pressure Δq. Thus (29) and (30) is written as

$$\Delta U = V(r/a)V^*(a,E,h\, q_0, \Delta q) , \tag{31}$$

$$\Delta w = G(r/a)\, G^*(a,E,h\, q_0, \Delta q) , \tag{32}$$

where

$$V(r/a) = \frac{r}{a}\sum_{i=0}\left(\frac{r}{a}\right)^{2i} b_1^{1-3i}\, d_i, \quad V^* = \frac{1}{a}\left(\frac{a^4}{2Eh}\right)^{\frac{2}{3}} [(q_0 + \Delta q)^{2/3} - (q_0)^{2/3}] , \tag{33}$$

$$G(r/a) = \sum_{i=1}\left(1-(r/a)^{2i}\right) b_1^{2-3i} c_i^*), \quad G^* = \left(\frac{a^4}{2Eh}\right)^{\frac{1}{3}} [(q_0 + \Delta q)^{1/3} - (q_0)^{1/3}] . \tag{34}$$

The numerical results obtained with the use of the formulas (31) and (32) for the mirror, which parameters are shown in table 6.1 at $q_o=0$ and $q=120$torr (0.163 atm) give $V^*=0.169$mm, $G^*=2.05$mm. Fig.6.1 shows the functions *V(r/a)* and *G(r/a).*

Table 6.1. *Parameters of the film.*

Thickness, h	Mirror radius, a	Young's module, E	Poisson's ratio, ν
80μm	25mm	460 kg/mm^2	0.3

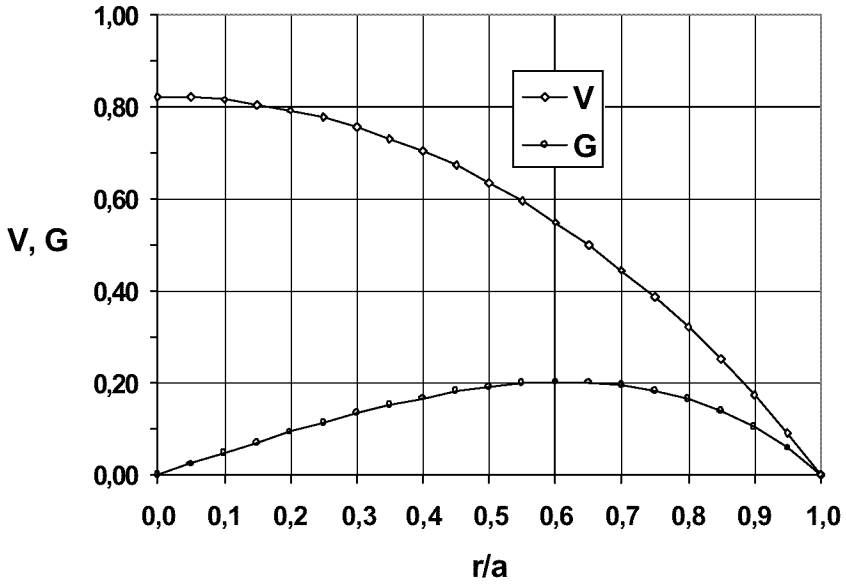

Fig.6.1. Functions *V(r/a), G(r/a).*

It is seen in Fig.6.1 the maxima of functions *V(r/a)* and *G(r/a)* are

$$V_{max} = 0.202\ ,\ G_{max} = 0.823 \tag{35}$$

The maximal shifts in the longitudinal and the cross directions are determined as follows

$$\Delta U_{max} = V_{max}\, V^{*}(a,E,h\, q_0\, ,\Delta\, q)$$

$$\Delta w_{max} = G_{max}\, G^{*}(a,E,h\, q_0\, ,\Delta\, q) \tag{36}$$

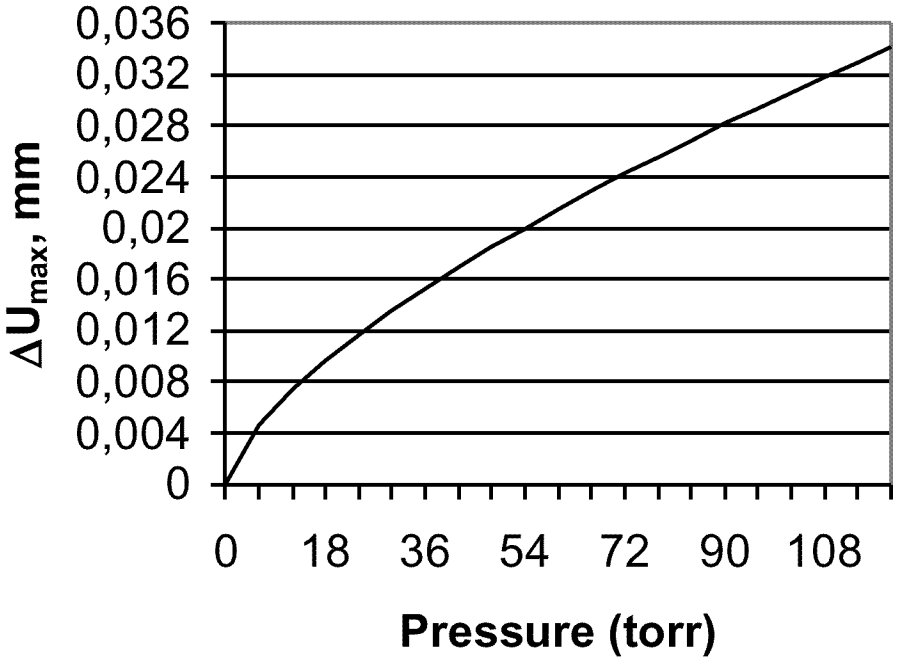

Fig.6.2. Dependence of ΔU_{max} on Δq at $q_o=0$.

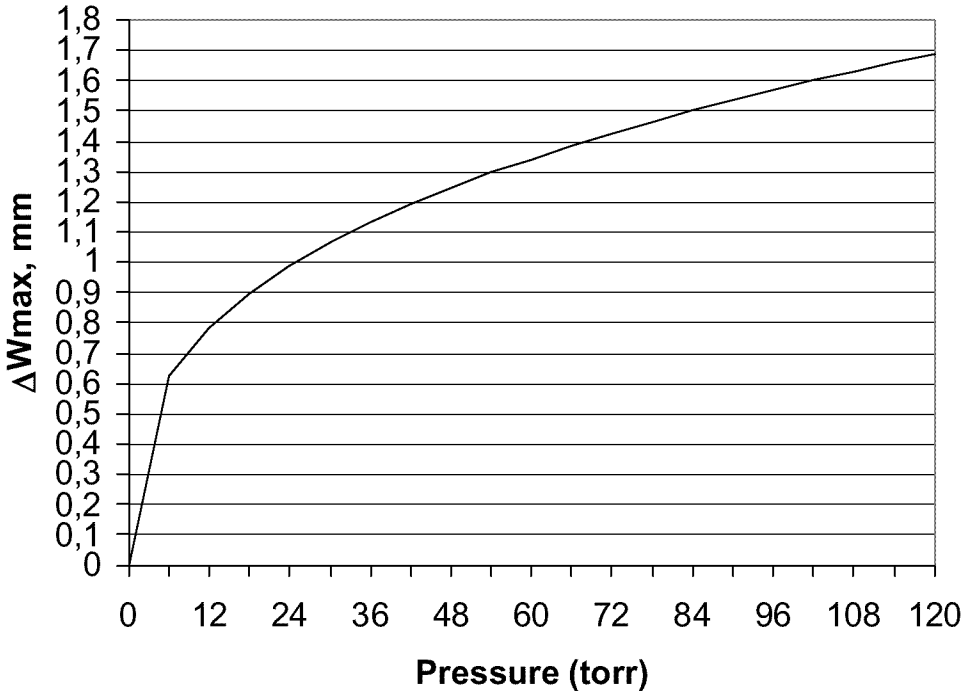

Fig.6.3. Dependence of Δw_{max} on Δq at $q_o=0$.

The maximum displacements of the film are monotone increasing ones with increase of Δq (see Fig.6.2 and Fig.6.3).

The functions exhibited in Fig. 6.1-6.3 correspond to the case of DOE applied on a plane membrane mirror, that is the case $q_o=0$. If the DOE is applied on a spherical mirror, as it results from the calculations, the distortions caused by mirror deformations maintain their appearance similar that shown in Fig.6.1. The corresponding functions of maximal distortions depending on Δq is shown in Fig.6.4 for the DOE applied on a concave mirror at $q_o=100torr$. Fig.6.5 shows the maximal shifts of the diffraction structure lines depending on pressure q_o (and hence on the initial mirror curvature) at constant Δq. It results from the calculations that the DOE distortions are maximal in the case of the flat mirror surface at pressure change Δq being the same. For the DOE applied on a spherical mirror being under pressure, e.g. $q_o=100torr$, the maximal shifts of the diffraction structure lines in the membrane plane and along the normal are, respectively, 4 and 1.7 times less than those at $q_o=0$.

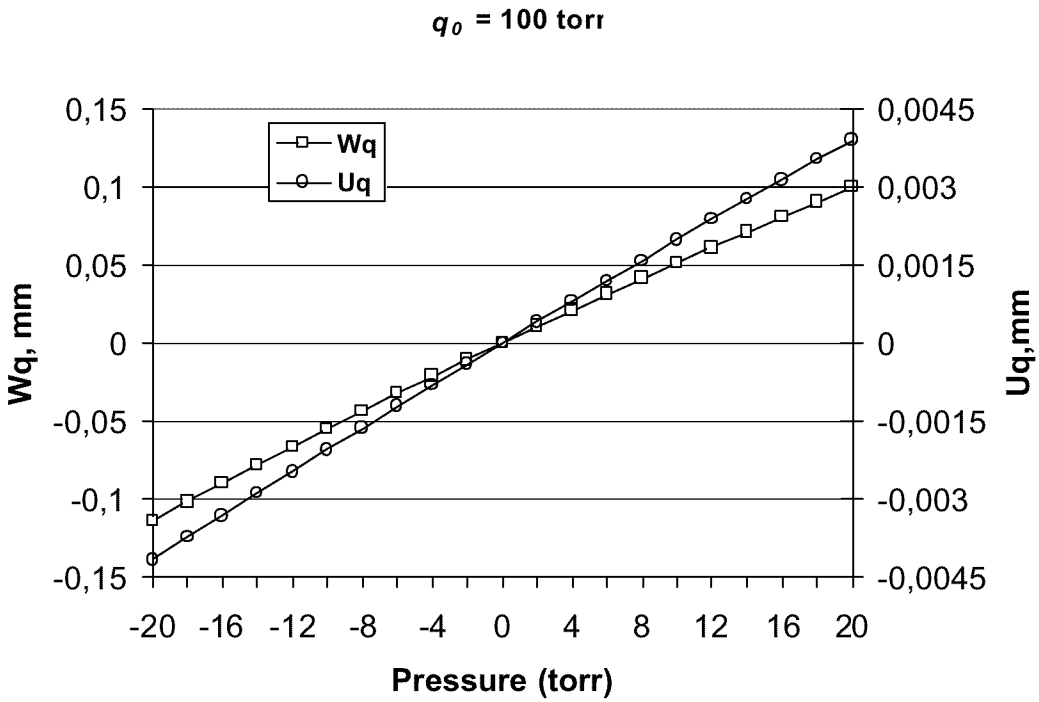

Fig.6.4. Dependence of ΔU_{max} and Δw_{max} on Δq at $q_o=100torr$ *(0.136 atm).*

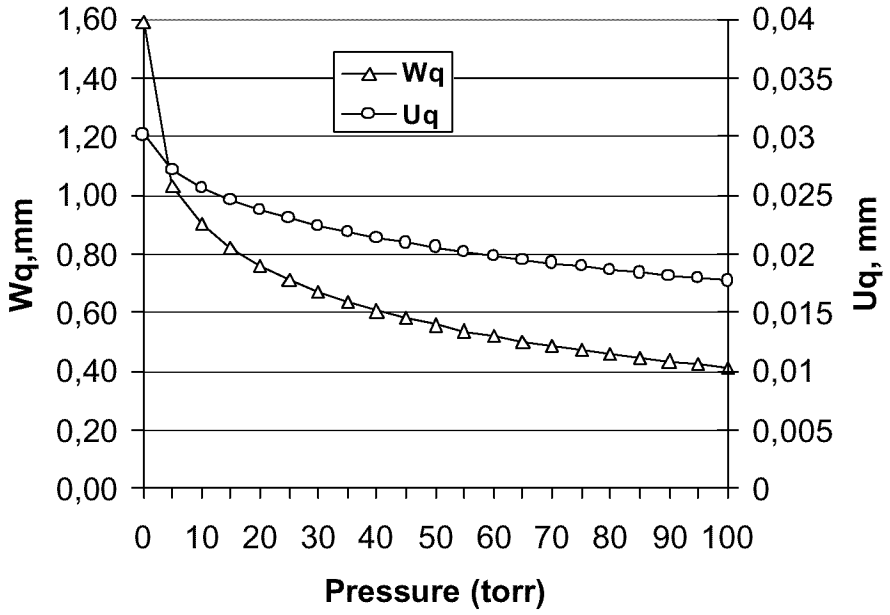

Fig.6.5. Dependence of ΔU_{max} and Δw_{max} on q_o at Δq =*100torr*

After the pressure has been applied the circles positions in the diffraction structure on the mirror surface change due to the shifts of mirror-surface points. Then an additional phase distortion in the beam diffracted on the distorted DOE is determined by the expression (valid in the paraxial approximation at $n>>1$ and $\Delta U(x_n)>>x_n$)

$$\varphi = \lambda \frac{\Delta U(x_n)}{x_{n+1} - x_n}, \qquad (37)$$

where $x_n = \sqrt{\lambda f n}$ is the n-th Fresnel's zone radius in the interference pattern of the plane wave and the diverging one of the curvature radius f, and λ the wavelength of these waves.

Fig.6.6 shows function φ of x.

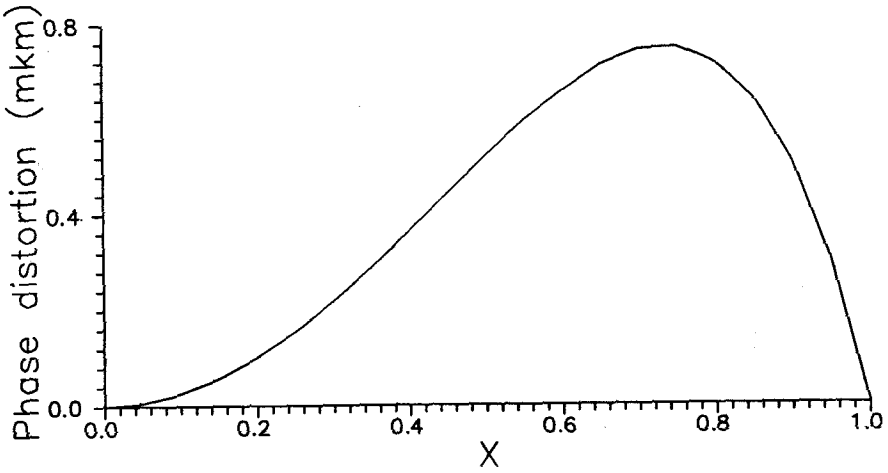

Fig. 6.6. Phase distortion brought by DOE in its minus-first-diffraction-order beam at q_o=0 and Δq=120torr.

The capacity-for-work conditions for a static diffraction structure on the deformed mirror are defined via the required image quality of observed objects. It is convenient to define the quality characteristic in a wave measure, for example, so that the residual distortions due to a DOE deformation are to be allowable ones if $\varphi_{max}<\lambda/2$. As results from (37) this condition is equivalent to

$$\Delta U(r, q_0, \Delta q) < 0.5\sqrt{\lambda f n} \tag{38}$$

Thus, the presented results of the theoretical analysis of deformation peculiarities of the static DOE on the membrane mirror have shown a curvature variation of such a mirror to lead to local transverse deformations of the film. This is followed by the shifts of DOE lines, and consequently by additional phase distortions in the reading out beam. The magnitude and the character of these distortions depending on the membrane mirror parameters have been determined. Along with this, the formulas have been deduced allowing one to determine the allowable both pressure and mirror's curvature variations in every concrete case.

6.2. Experimental study of stability of static DOE on the membrane mirror surface

The experimental investigation of stability of the static DOE on the membrane mirror surface was conducted to verify the results of the theoretical analysis of elastic-film-deformation peculiarities in the real experimental conditions. The matter is that the theoretical consideration concerned the elasticity task of axial symmetry. Thus the film characteristics were assumed to be uniform and the forces to be constant along the azimuth coordinate. The earlier experiments on investigation of elastic mirror optical quality showed that it was fairly difficult to attain axial symmetry for the surface shape of the real mirror. Non-uniformity of mechanic features of the film being at our disposal required the special adjustment facilities in the mirror-mounting construction to even azimuth film deformations. However we could not yet eliminate the distortion asymmetry. In this regard we had to analyze in what measure the theoretical consideration results can be applied to available distortions of the experimental mirror surface.

6.2.1. Fabrication of samples of membrane mirrors with static DOE

As the first attempt to fabricate DOE was tried the ablation method. This method comprises partial elimination of some pieces of the reflecting surface by exposure them to high power laser irradiation. The experimental layout is shown in Fig.6.7. The beam from YAG-Nd+3 laser 10mm in diameter was split into two beams by a beamsplitter BS1, and the interference pattern was recorded in the plane of the pan with an aluminum 20μm thick film stretched on it.

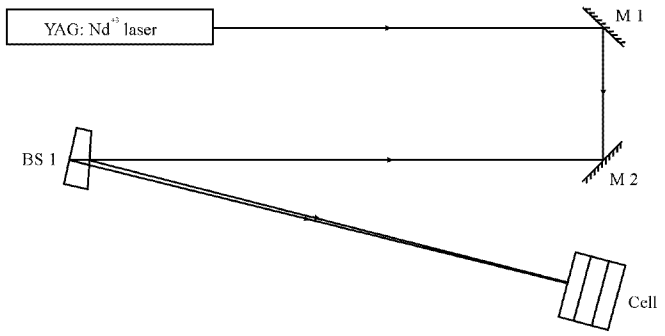

Fig.6.7. Schematic of the experimental setup for ablation method.

The experiments carried out resulted in the acceptable regimes of the ablation process. Fig. 6.8(a, b) illustrates the ablation process threshold (a), and the dynamic range of exposure (b).

a) b)

Fig.6.8. Illustrations of the different regimes of the ablation process:
a) Pump energy 11kJ, pulse duration 300 μs;
b) Pump energy 7kJ, pulse duration 300 μs.

It is seen that the laser beam power providing the distinct lines of the interference pattern can be chosen. However this method possesses some essential drawbacks:

- a narrow band of the allowable exposure;
- high requirements to film characteristics and to uniformity of the beam intensity across its section;
- a low resolution of the blurred grating at small angles between the crossover beams.

The ablation process of an aluminum layer is non-uniform in nature. So it requires further studying for successful fabrication of the DOE on the membrane mirror surface.

Therefore, we employed other techniques for our purpose.

To carry out the experiments we have fabricated several types of the membrane mirrors with the static DOE. The simplest mirrors were fabricated from the photo-film which surface after special processing was coated with the reflecting aluminum layer. In this case the DOE was recorded as a relief hologram on the mirror. Along with this, the mirror samples were fabricated with the layer of a nonlinear medium applied on the specular surface of the film. Recording DOE on the photo-film and in the nonlinear medium was executed with the use of appropriate coherent laser beams. In addition, the membrane mirror sample was fabricated from the photo-film with the computer- synthesized DOE.

Fig.6.9 shows schematic of the tabletop setup for recording DOEs by laser beams.

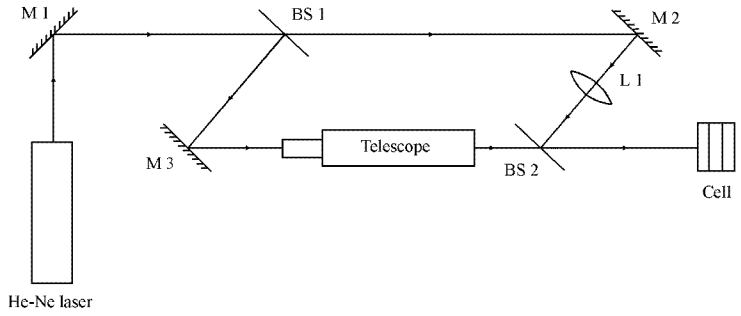

Fig. 6.9. Schematic of the setup for recording DOE.

The beam of He-Ne or Ar laser of power of either15mW or 200mW, respectively, was split by the beam-splitter BS1 into two beams. One beam (transmitted through the beam-splitter BS1) was reflected by the flat mirror M2, focused by the high quality objective L1 with the focal length of 50mm, then reflected by the beam-splitter BS2, and hit upon the photo-film placed in a pan or in the special mounting of mirror. The curvature radius of this beam in the film plane was 1.17m. The other beam (reflected from the beam-splitter BS1) having been reflected by the flat mirror M3 was broaden by a collimator up to diameter of 50mm, then passed through the beam-splitter BS2, and hit upon the photo-film as well. In the plane of the photo-film there was formed the interference pattern of these two beams. The number of its lines amounted to 45 mm^{-1} at the DOE edge. The beam intensities were matched with the use of the light filter.

The having been exposed photo-film was developed and fixed. The hologram obtained was transmitting and amplitude-phase-relief in nature. The main contribution in its diffraction efficiency was of its amplitude component. Table 6.2 presents the measured parameters of this hologram (see column 'amplitude'). The film was bleached, and then the diffraction main contribution became already of the phase component (column 'relief' in table 6.2). All

processing operations (developing, fixing, bleaching, and deposition of an aluminum layer) were as a rule executed without taking off the film from the mirror mounting.

??????? 6.2. The static-DOE parameters of the fabricated samples.

	PHOTOGRAPHIC TECHNIQUE			COMPUTER TECHNIQUE		
	Amplitude	Phase	Relief	Amplitude	Phase	Relief
Diffraction Efficiency (%)	0.86	6.7	14.4	7.2	8.3	3.2
Transmittance for zero diffraction order (%)	4	9	0.85	18	11.6	4.6

One of the ways to fabricate the static DOE was chosen the computer synthesizing. Presently a lot of computer programs exist which allow design of the required hologram to be corresponding to the given formula. Such a pattern is then printed with the use of a photo-printer having maximum resolution 5000 dpi (≈30 lines per mm). A laser printer can be employed as well but its maximum resolution being less than that of the photo-printer amounts to only 1600 dpi (≈10 lines per mm). Such a technology can be apparently used in the future with the appropriately updated printers.

For the experiments we have fabricated with this technology the DOE 50mm in diameter on a 110-μm thick mylar film. The number of lines at the DOE edge amounted to 50 mm^{-1}, the focal length of the DOE being 0.8m. The hologram obtained was a transmitting one of an amplitude type. Fig.6.10 shows the minus-first diffraction order intensity distribution in the focal plane of the DOE.

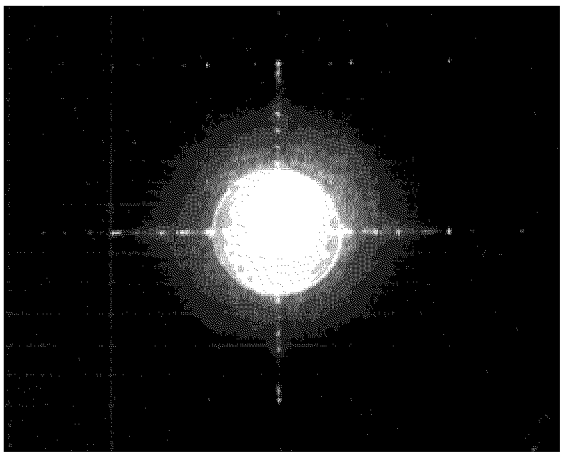

Fig.6.10.
The minus-first-diffraction-order intensity distribution in the focal plane of the computer synthesized DOE.

Then we bleached and coated this sample with aluminum.

It is seen in Fig.6.10 that there are noise components. It resulted from that the line density of the DOE exceeds the resolution-capability of the photo-printer used. Therefore the DOE has got so called 'ghosts' looking like weak concentric circles. It is they are seen in the figure as a noise.

Table 6.2 presents the measurement results for the computer synthesized DOE. As is seen the relief hologram obtained with the use of the photographic method has the maximum diffraction efficiency ~14.4%, whereas the phase hologram based on the computer technique ~8.3%. The hologram transmission in zero diffraction order does not exceed 9% and 18% for the respective DOEs. These results evidence for necessity of additional studies aimed at selection of the films having minimal absorption and light scattering, at optimization of technological processing, and at lowering diffraction efficiency for other (excluding minus-first) diffraction orders of the DOE by means of profile variation of its lines.

The optical distortions acquired by the beam transmitting the film were examined through an interferometer with a plane-front reference beam. Its schematic is shown in Fig.6.11.

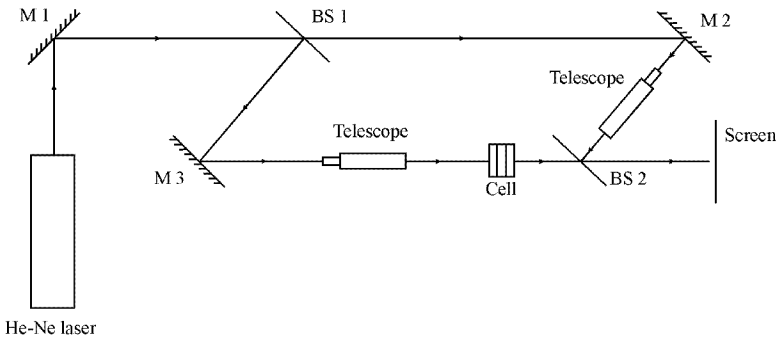

Fig.6.11. Schematic of the interferometer for examination of the film optical distortions.

The film was fixed in the special mounting which construction allowed changing of the membrane-curvature radius by pumping off the air from its inner volume. Fig.6.12 presents the obtained interferograms for the case of the film fixed not being under a pressure load (Fig.6.12,a) and the film being under pressure P=150torr (Fig.6.12,b). The distance between the adjacent lines of the interference pattern corresponds to the phase change of 0.6328μm. As is seen in Fig.6.12,a the film in its initial state is not uniform and brings distortions up to 0.4μm in magnitude with their characteristic scale of about 1 cm. The film deformations caused by external pressure of 150torr virtually do not change the distortions considered (Fig.6.12,b).

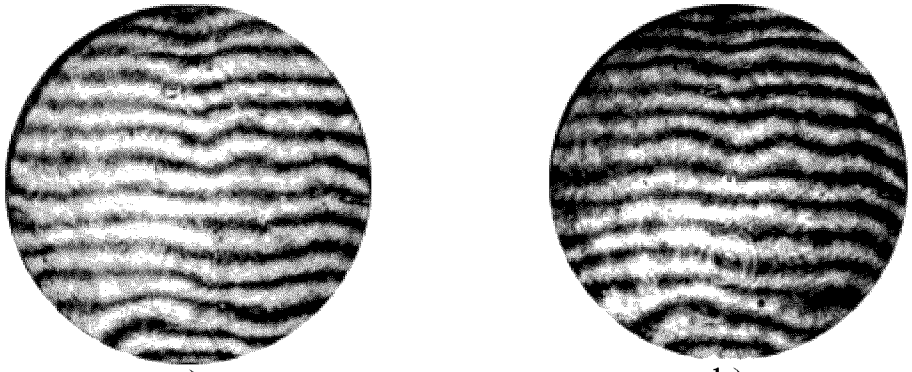

Fig.6.12. Interferograms of the film in the transmitted beam:
a) at P=0; b) at P=150torr.

6.2.2. Investigation of static DOE stability

The static-DOE-stability study was carried out basing on both the focal spot and interference techniques for the transmitting and reflecting DOE fabricated samples. In the experiments two laser beams were simultaneously directed on the DOE being under study (see Fig.6.13).

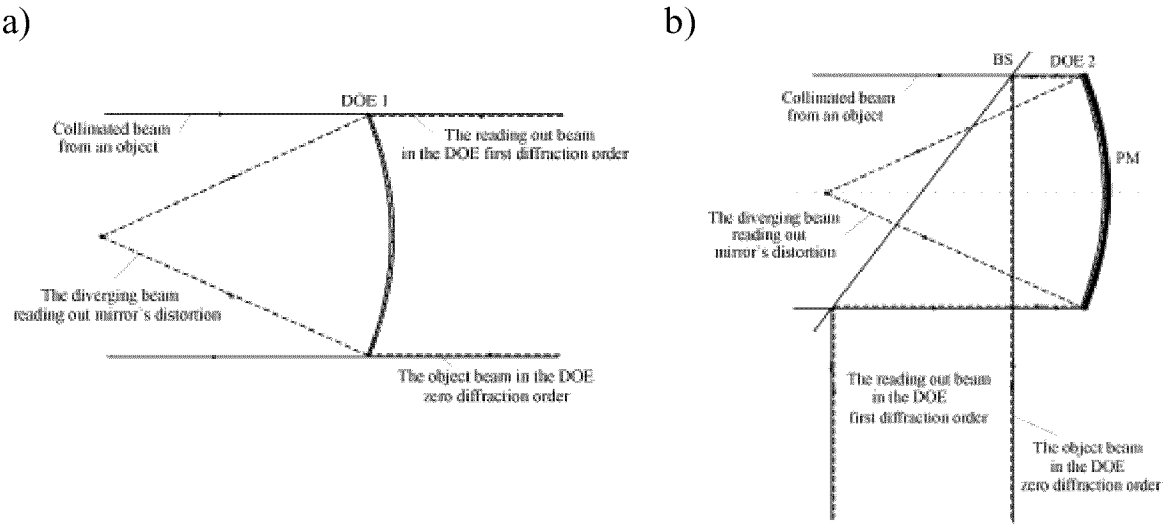

Fig.6.13. Principal ideas of the study of static DOE:
a) transmitting DOE; b) reflecting DOE.

One of the beams (collimated) simulated the beam from an observed object to be reflected from the PM (with DOE) in zero diffraction order. The other beam (diverging) having been diffracted in the DOE minus-first-diffraction order, inquired the distortions of the mirror and then (after passing the DOE) propagated in that same direction as the above beam done. The focal intensity distributions of these beams were analyzed, and their interference pattern was registered (In this case the beams incident on the DOE were coherent.) The distortions conditioned by DOE instability led to different non-identical focal distributions and to deformations of the interferogram lines. It should be noted that the interference method provided substantially higher measurement accuracy than that above due to its insensitivity to either the film non-uniformity (the case of transmitting DOE) or defects of the mirror shape (reflecting DOE).

The optical schematic of the experimental setup is shown in Fig.6.14. This scheme allows one to study transmitting as well as reflecting DOEs. We employed it with the use of the high-quality 100mm-diameter objective L2 of focal length of 250 mm in the case of the reflecting DOE. In the case of transmitting DOE there was employed the diffraction-order selector looking like a 1mm-diameter diaphragm 4 in the focal plane of objective L3.

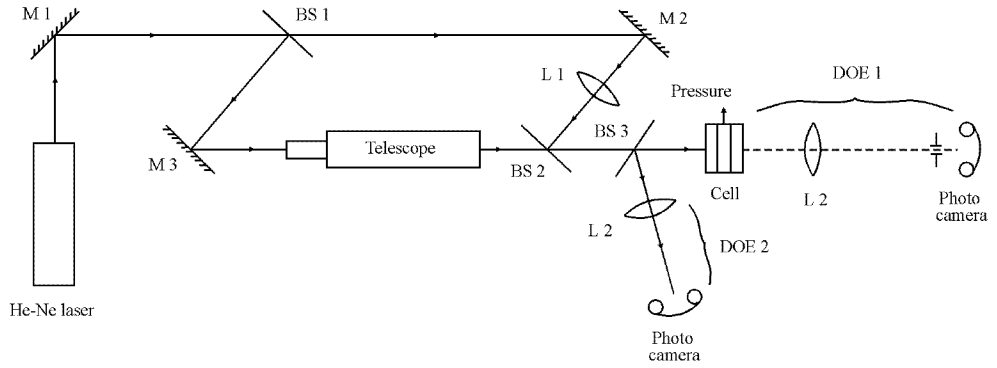

Fig.6.14. Optical schematic of the setup for the study of static DOE stability.

Fig.6.15 presents the main measurement results such as interferograms and focal intensity distributions for the transmitting phase DOE applied on the 85μm thick mylar film at different applied pressures. The results in Fig.6.15 were obtained in the absence of the applied pressure, namely, in the conditions of recording the DOE. As is seen, the interference lines are virtually rectilinear and the corresponding focal spots are identical to one another. With increasing the pressure up to 90torr the distortions in the interference pattern become appreciable (Fig.6.15, c,d), at P=150torr in addition the distortions in the focal spot become to be visible (Fig.6.15 e,f).

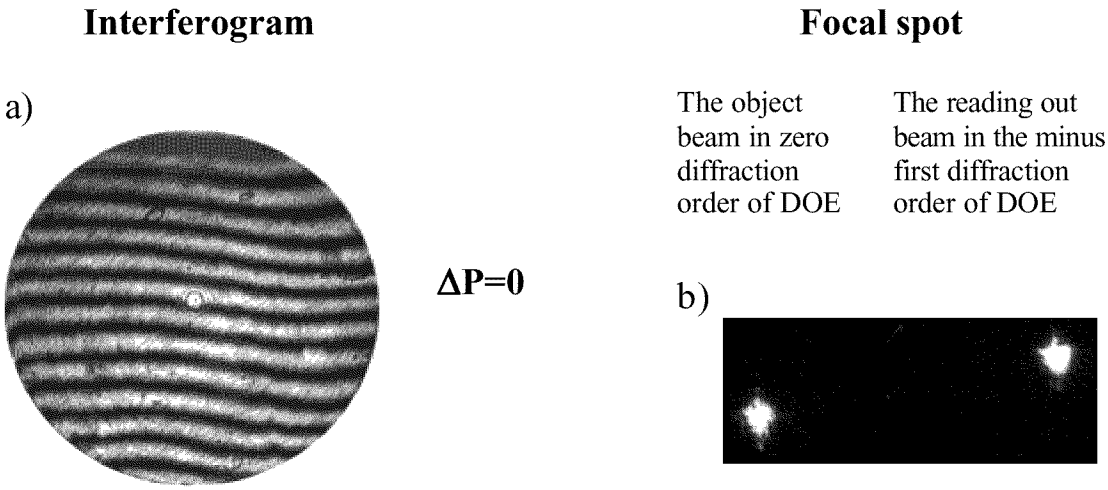

Fig.6.15. The measurement results for the transmitting phase DOE.

Section 7. Comparative analysis of applicability of dynamic and static DOE on large aperture membrane mirrors

In the previous sections of this report the main results of the theoretical and experimental studies of peculiarities of fabrication and functions of static and dynamic DOEs on membrane mirrors have been described. There were considered the optical schemes for recording the DOEs, presented the survey of nonlinear media suited for recording dynamic DOEs, and also the results of the experimental examinations of the samples of the membrane mirrors having a static or dynamic DOE on their surfaces. In this section we present the results of a comparative analysis of advantages and drawbacks of static and dynamic DOEs in application to large aperture membrane mirrors.

Static DOEs seem to be attractive first of all for easy technology of their manufacture. The membrane mirror with such a DOE may be fabricated in lab conditions, tested, certified and then sited in a real imaging system. After the system operation has been inspired as a whole, the mirror is transported to its working place, for instance, on a near-earth orbit of some satellite. An advantage of the static DOEs is that it is fabricated on the Earth under accurately controlled conditions.

The manufacture process of static DOEs has been well developed now. Several technologies are known to allow embodying of sufficiently large scale DOEs. These are first of all classic photography and holography methods of recording distortion information, photolithography, computer holography and others. Note also that there exist a lot of nonlinear media for recording static DOEs on membrane substrates such as silver and other emulsions, polymer films, reoksan, photoresists and so on. When following the proper technological conditions of processing one can get DOEs with virtually unlimited durability in normal operation conditions.

The main disadvantage of static DOEs is the following one. The surface distortions of the membrane mirror with the DOE, those ones to be further compensated by a correction system, lead in turn to deformations of the DOE. So when information on mirror's distortions is read out, the additional aberrations arise conditioned by imperfection of the DOE. These aberrations are not compensated in the correction system and down the image quality of an observed object. In Section 6 of this report the main results of the theoretical and experimental studies of DOE deformations and their effects on the image quality are presented. The range of the allowable mirror's distortions providing the required image quality is shown to be a function of mirror's parameters. So, the static DOEs limit the range of the compensated mirror's distortions. This is an essential drawback of static DOEs as compared with dynamic ones.

Note that this drawback can be partly eliminated if the mirror with the static DOE is designed according to the known scheme [57] in which the DOE is

formed in an additional film placed in front of the mirror and unexposed to the mirror's pressure load.

When the static DOEs are used it is necessary precise alignment of the scheme for its correct operation. The allowable errors in the mutual positions of the optical elements have not to exceed portions of the spatial period of the DOE's holographic grating at the mirror edge. For large scale mirrors and operation in the visible and near IR wavelength range it becomes difficult to meet these requirements. For this reason the employment of static DOEs on segmented mirrors if the segments and DOEs are manufactured separately appears to be impossible or at least extremely difficult.

A limitation exists for the maximum size of the membrane mirror with the static DOE applied to its surface. This limitation is conditioned by requirements to parameter stability of the film being the mirror substrate, to uniformity of the nonlinear medium applied on the film, to stability of technological process and so on. Nowadays the maximum size of such a mirror with the DOE is limited by about 1m.

The dynamic DOEs as well as the static ones possess a number of rather attractive features. These features become apparent to the utmost when the dynamic DOEs are chosen for operation in the telescopes with large-clear-aperture primaries. For example, the fact, that the dynamic DOEs re-adjust for the primary mirror distortions during the operation so that their diffraction structure follows the mirror shape, allows the dynamic DOEs to compete successfully against the static ones.

This subject is especially important in the imaging systems with segmented primaries since the dynamic DOEs are even not critical in respect to step-wise defects of the mirror surface and not only to its smooth distortions. Therefore the dynamic DOE applied on the segmented primary mirror provides automatic matching of the grating lines at the segment's edges at their arbitrary positions. On the contrary, to attain this with the use of static DOEs is an extremely difficult task. Thus, employment of dynamic DOEs eliminates or at least downs the limitations related to the above subject on enlarging the primary mirror dimensions. So, the dynamic DOEs can be helpful in the segmented-design imaging systems having the correctors for PM distortions.

However, the dynamic DOEs are not free from drawbacks and their usage causes some additional problems as compared to the static DOEs. First of all note the serious sophistication of the imaging-system optical scheme due to introduction of the additional technique for recording the dynamic DOE. Such a technique that has to function continuously and correctly in conditions of the telescope exploitation is to meet high requirements. These in turn lead to enlarging the system mass and dimensions as well as the cost. In addition reliability of the system as a whole reduces.

Continuous resumption or maintenance of the dynamic DOE optical parameters requires solution of some additional technical problems, for example,

such as energy supply, keeping of temperature regime of the system as a whole and in particular of its primary with the dynamic DOE. An important problem for the dynamic DOE appears to be its limited durability determined for some nonlinear media as an amount of record/read cycles. Obviously, the dynamic DOEs are out of competition in large-scale single-shot telescopes, for example, such as a projecting telescope.

Nowadays an especially important problem of employment of the dynamic DOEs is that the stock list of nonlinear media to meet in a sufficient measure high complex requirements of the systems having the large aperture primaries is fairly limited.

These requirements involve the combination of several poorly compatible features. For example, high sensitivity to the recording light and insensitivity to the reading light are to be met simultaneously. The material must show uniform response characteristic in both the high and low spatial frequency range and be tolerant to a wide range of environments conditions (temperature, pressure, operation in vacuum etc.).

A serious problem of choice of the nonlinear media for the dynamic DOEs is that of their temporal characteristics. To compensate successfully for the dynamic distortions of the primary mirror it is necessary to have the characteristic times of recording, free relaxation and forced erasing being in specific relations with each other as well as with temporal characteristics of the compensated distortions. For instance, for a pulse-repetitive record/read mode it is needed the temporal relations

$$\tau_{rec}+\tau_{erase}<<\tau_{read}, \qquad \tau_{rec}+\tau_{read}+\tau_{erase}<<\tau_{def},$$

Here τ_{rec}, τ_{read}, τ_{er}, are the characteristic times of recording, reading out, and erasing of the DOE, and τ_{def} of deformation of the mirror surface. As a rule the real nonlinear media hardly meet combinations of several various requirements.

It is very important now the development of technologies which do not exist yet of application of the uniform layers of nonlinear materials on the working surface of a large aperture membrane PMs.

Table 6.3 and 6.4 summarize the main advantages and disadvantages of dynamic and static DOE applied on the membrane mirror surface.

Table 6.3.

Dynamic DOE	
Advantages	Disadvantages
1.No additional optical distortions following the mirror distortions. 2. Limitation of the mirror distortion magnitude is determined by the system optical elements rather than by DOE. 3. Weak limitations of the PM size and possible segmented designs.	1. Continuous maintenance of dynamic DOE: - energy supply - heat off - stability of light sources. 2. Limited durability. 3. Sophistication of the telescope scheme due to the additional technique of recording the dynamic DOE. 4. The problem of simultaneous meeting the parameter requirements (dynamics, sensitivity…) for the low and high spatial frequencies of the hologram. 4. The limitations in the process dynamics: $\tau_{rec} < \tau_{read} + \tau_{obser} < \tau_{def}$

Table 6.4.

Static DOE	
Advantages	Disadvantages
1. Single-shot fabrication. 2. Wider technology and material area. 3. Higher diffraction efficiency as compared with dynamic DOE. 4. Unlimited durability. 5. The modified version exists of the mirror with static DOE on an additional film not being under pressure.	1.DOE structure is deformed simultaneously with the mirror deformations. 2. Precise adjustment is needed for correct operation. 3. Limitations exist of the mirror distortions for DOE's correct operation. 4. It is impossible or extremely difficult to use static DOEs on the surface of segmented mirrors. 5. Limitations exist on the static-DOE maximum size (presently about 1m).

Conclusions

Presently the technologies of dynamic and static DOEs applied on membrane mirrors are being developed. It is prematurely to decide conclusively what method is the preferable one. The choice may be done only for a concrete application with clear-cut requirements to the system as a whole and to the PM in particular. The telescope with the static DOE all other things being the same has

benefit in its mass and dimension characteristics as well as in energy consumption.

As regard to large aperture membrane mirrors it should be noted that the static DOEs are easier in realization but their application area is limited, and dynamic DOEs are more universal but more complicated in realization.

References

1. Final Report on the Contract F61775-98-WE089 (project SPC-98-4065) "Nonlinear-optical correction of aberrations in imaging telescopes based on a diffraction structure on the primary mirror").
2. Dimakov S.A., Gorlanov A.V., Kislitsyn B.V., Zhuk D.I., "Upon feasibility of application by laser radiation for static diffraction optical element on the surface of a thin film mirror", Proc. SPIE, vol. 3785, July 1999, p. 130-139.
3. S.N. Koreshev, Optika i Spektr., 76, N1, pp. 109-115, 1994 (in Russian).
4. Phys.Rev.Lett.66,1846(1991).
5. P.N. Prasad, M.E. Orczyk, J. Zieba, R. Burzynski, Y. Zhang, S. Ghosal, M. Casstevens, Polymeric composite photorefractive materials for nonlinear optical applications, SPIE v.2143, pp. 80-87 (1994).
6. B. Kippelen et al., "Infrared photorefractive polymers and their applications for imaging", Science 279, 54 (1998).
7. Jon A. Herlocker, Kyle B. Ferrio, Eric Hendrickx, Brett D. Guenther, Stephane Mery, Bernard Kippelen, Nasser Peyghambarian, "4-ms response time in a photorefractive polymer", Proc. SPIE, v. 3623, pp.168-174 (199?).
8. E. Marom, V. Efron, Optics Lett. 12 (1987) 504.
9. A. Januszko, A. Miniewicz, Adv. Mat. Opt. Electron. 6 (1996) 272.
10. W. M. Gibbons, P. J. Shannon, S. T. Sun, B. J. Swetlin, Nature 351 (1991) 49.
11. A. G. – S. Chen, D. J. Brady, Optics Lett. 17 (1992) 441.
12. I. C. Khoo, H. Li, Y. Liang, Optics Lett. 19 (1994) 1723.
13. I. C. Khoo, H. Li, Y. Liang, Optics Lett. 20 (1995) 130.
14. I. C. Khoo, IEEE Quantum Electron. 32 (1996) 525.
15. H. Ono, N. Kawatsuki, Optics Comm. 147 (1998) 237.
16. V.P Pham, G.Manivannan, R.A.Lessard, "Real-time dynamic holography using azo-dye doped PMMA based recording media", SPIE v.2405, pp.133-142 (1995).
17. D.L.Ross and J.Blanc, in "Photochromism",G.H.Brown, Ed., Chap.5, John Wiley and sons, New York, 1971).
    H.Rau, in "Photochromism", H.Durr and H.Bouas-Laurent, Eds.,p.165, Elsevier, Amsterdam, The Netherlands,1990.
18. F.Tatezono, T.Harada, Y.Shimizu, M.Ohara and M.Irie, Jpn. J.Appl. Phys., 32,pp.3987-3990(1993).
19. Roger A. Lessard, Gurusamy Manivannan, "Photochromism used in holographic recording", SPIE v.3347, pp.11-19 (1998).
20. Sehwerzel R.E. The Spectrum,6,1(1993).
21. Zhao M.T., Samos M., Singh B.P., Prasad P.N., J.Phys.Chem., 93, p.7916 (1989).
22. S.M. Maloletov, A.S. Kutzenko, A.A Borshch, M.S. Brodyn, O.M. Buryn, V.I. Volkov, "New epoxy-based linear polymer as recording medium for transient holography", SPIE v.2688, pp. 70-81 (1996).

23. A.A Borshch, M.S. Brodyn, O.M. Buryn, V.I. Volkov, A.S. Kutzenko, S.M. Maloletov, "Effective dynamic and stationary hologram recording in new epoxy-based polymers", SPIE v.3294, pp. 99-104 (1998).
24. Eltsov A.V., Bren V.A., Gerasimenko Yu.E. et al. J.Appl.Phys., 69,8011(1991).
25. Hillet J. J.Physics and photochemistry of polymers (M.,Mir,1988).In Russian.
26. Barachevsky V.A., Lashkov G.I. Photochromism and applications (M.Chimia,1977) In Russian.
27. Sean X. Wu, Ching-Shan Cheng, Tizhi Huang, Shaowen Qin, James J. Yeh, Qiang Gao, Alan G.Chen, Chao-Pin Yeh, Austin Harton, Karl Wyatt, "Experimental study on mechanical, thermomechanical, and optomechanical behaviors of holographic materials, SPIE v.3294, pp.145-151 (1998).
28. Optical and electrical properties of bacteriorhodopsin Langmuir-Blodgett films. Howard H. Weetall, Lynne A. Samuelson. Thin Solid Films. 1998. ? 312. p. 306-312.
29. Elements of a unique bacteriorhodopsin neural network architecture. Dan Haronian, Aaron Lewis. Appl. Opt. 1991. v. 30, ? 5. p. 597-608.
30. Transverse optical effects in bistable active cavity with nonlinear absorber on bacteriorhodopsin. V.Yu. Bazhenov, V.B. Taranenko, M.V. Vasnetzov. Proc. SPIE. 1991. v. 1840, Transverse Patterns in Nonlinear Optics. p. 183-193.
31. Bacteriorhodopsin-based single and dual wavelength holographic interferometry for monitoring crystal growth. Colleen Fitzpatrick, Ching Mei Yang, Dominique Fourguette. Opt. Eng. 1998. v. 37, ? 6. p. 1708-1713.
32. Kinetics of formation and relaxation of dynamic gratings in conditions of saturated photo-response in reversible light-sensitive media. Yu. O. Barmenkov, N.M. Kozshevnikov. Opticheskiy Zhournal, 1997, v.64, ? 4, pp.106-110.
33. Influence of photochemical transformation dynamics on interaction of light waves in bacteriorodipsin based media. V.B.Kotov, Radiotechnika i elektronika, 1997, v.42, ? 7, pp.871-877.
34. The intensity dependent refractive index change of photochromic proteins. V.P. Leppanen, T.J. Haring, T. Jaaskelainen, E. Vartiainen, S. Parkkinen, J.P.S. Parkkinen. Opt. Commun. 1999. ? 163. p. 189-192.
35. Serey Thai, "Laser-induced M-state holographic gratings of a hydrated D96N bacteriorhodopsin film", SPIE v.3638, pp.35-40 (1999).
36. Akimov I.A., Denisyuk I.Yu., Kislovsky I.L., Meshkov A.M., Phototermoplastic film for air-cosmic observation apparatus, Opticheskiy Zhournal, 1993, ? 12, pp.65-71.
37 Akimov I.A., Denisyuk I.Yu., Kislovsky I.L., Meshkov A.M., Physics of high-sensitive consecutive PTP process// Opticheskiy Zhournal, 1996, ? 4, pp.49-56.
38. Cherkasov Yu.A., Alexandrova E.L., Roumyantzev A.I., Smirnov M.V., Investigation of kinetics of formation of photothermoplastic relief-phase

images and feasibility analysis of adaptive registration of images// Optichesky Zhournal, 1996, ? 4, pp.77-87.
39. Cherkasov Yu.A., Alexandrova E.L., Roumyantzev A.I., Smirnov M.V., Development of dynamic model of photothermoplastic relief-phase image formation for realization of adaptive registration ideology.// Optichesky Zhournal, 1996, ? 4, pp.88-95.
40. Akimov I.A., Denisyuk I.Yu., Meshkov A.M., Nano-structured photo conductors are novel media for electrophotographic and photothermoplastic materials// Optichesky Zhournal, 1996, ? 4, pp.69-76.
41. Denisyuk I.Yu. Application of transporting thermoplastic PTP-material layer by means of electrostatic deposition// Optichesky Zhournal, 1996, ? 4, pp.61-64.
42 H.W. Kroto et al., Nature 318, 162 (1985).
43. V.N. Bezmelnitzin, A.V.Eletzky, M.V.Okoun, Fullerenes in solvents //Uspekhy Fiz Nauk, 1998,v.68,? 11,pp.1195-1219.
44. A.V.Eletzky, B.M. Smirnov. Fullerenes. //Uspekhy Fiz Nauk, 1993, v.163, ? 2, p.33.
45. I.M. Belousova, V.P. Belousov, E.A. Gavronskaya, et all. Fullerene-based nonlinear optical devices for fast control of spatial power and temporal characteristics of laser radiation. Proc. SPIE, 1998, 3682, 201-209.
46. V.P. Belousov, I.M. Belousova, V.P.Boudtov, V.V. Danilov, O.B. Danilov, et al. Fullerenes: structural, physical-chemical and nonlinear optical properties. Optichesky Zhournal, 1997, v.64, ? 12, pp.3-37.
47. V.P. Belousov, I.M. Belousova, V.G.Bespalov, V.P.Boudtov, V.M. Volynkin, V.A. Grigor'ev, O.B. Danilov et al. Nonlinear optical properties of fullerene doped media.// Optichesky Zhournal, 1997, v.64, ? 9, pp.82-84.
48. S. Couris. Fullerenes reveal their nonlinear optical traits. Proc. OLE, 1996, Sept., 63-64.
49. Y.N. Han, W.J. Zhang, X.M. Gao, Y.B. Cui, Y.X. Xia. Nearly resonant two-photon absorption of C_{60} thin film at 633 nm. Appl. Phys. Lett., 1993, 63, ? 4, 447-448.
50. V.P. Belousov, I.M. Belousova, O.B. Danilov, V.V. Danilov, V.A. Grigor'ev, A.G. Kalintsev, A.J. Sidorov. Nonlinear optical limiters of laser radiation based on reverse saturable absorption and stimulated reflection. Proc. SPIE, 1998, 3263, 124-130.
51. M.V. Gryaznova, V.V. Danilov, N.V. Kamanina. Opt. Journ. 1997, v. 64, ? 10, 15-116.
52. S.R. Mishra, H.S. Rawat, M.P. Joshi, I.C. Mehendale, K.C. Rustagi. Optical limiting in C_{60} and C_{70} solutions. Proc. SPIE, 1994, 2284, 220-229.
53. Y. Song, X. Ban, F. Li et al. Excited state absorption/random surface scattering limiter. Proc. SPIE, 1996, 2856, 216-219.

54. Kwanghee Lee, E.K. Miller,N.S. Sacriciftci, J.C. Hummelen, F. Wudi, A.J. Heeger. Nonlinear optical changes in conducting polymer-methanofullerene films evaluated by photoexcitation spectroscopy. Proc. SPIE, 1996, 2854, 199-207.
55. E.S. Maniloff, D. McBranch, H.L. Wang, B. Mattes. Charge transfer polymers: a new class of materials for nonlinear optics. Proc. SPIE, 1996, 2854, 208-213.
56. O.B. Mavritsky, A.N. Egorov, A.N. Petrovsky, K.V. Yakubovsky. Third-order optical nonlinearity of C_{60} and their metal derivatives under picosecond laser excitation. Proc. SPIE, 1996, 2854, 254-265.
57 S.A. Dimakov, B.V. Kislitsyn, "Analysis of the elasticity theory equations aiming to clear up main relationships of the parameters in the thin-flexible-mirror task" SPIE-3610.